FINAL REPORT: FADE ANALYSIS OF ORCA DATA BEAM AT NTTR AND PAX RIVER

UCF DARPA Project ID: 16296051

HR0011-08-C-0111

R. Crabbs, D. Wayne, T. Leclerc, and P. Sauer
Florida Space Institute (FSI), University of Central Florida,
MS: FSI, Kennedy Space Center, FL 32899

L. C. Andrews, R. L. Phillips
Consultants for ManTech Corporation, Arlington, VA

August 2010

This work was funded by the Defense Advanced Research Projects Agency (DARPA) in support of the Optical RF Communication Adjunct (ORCA) Project with Program Manager Dr. Larry Stotts. Distribution Statement "A" (Approved for Public Release, Distribution Unlimited).

SUMMARY

The DARPA Optical RF Communications Adjunct (ORCA) program was designed to bring high data rate networking to the warfighter via airborne platforms. Preliminary testing of the ORCA free-space optical communication (FSOC) laser beam was performed on May 12, 2009 by the Northrop Grumman Corporation (NGC) at Patuxent (PAX) River Naval Air Base in Maryland. Phase I testing of the ORCA system from/to an aircraft to/from a mountaintop was then conducted by NGC at the Nevada Test and Training Range (NTTR) located on the Nellis Air Force Range near Tonopah, NV. The University of Central Florida (UCF) was separately contracted by DARPA to measure path-averaged values of the refractive-index structure parameter C_n^2, the inner scale of turbulence l_0, and the outer scale of turbulence L_0 along the propagation path from the NGC BAC 1-11 aircraft to Antelope Peak during the ORCA testing at NTTR. The testing took place over May 16-18, 2009 and a Report on those measurements was submitted to DARPA in September 2009 [1]. Additional tasks assigned to UCF after the NTTR testing included further analysis of the aero-optic effects from the aircraft boundary layer, adaptive-optics (AO) compensation issues, and fade statistics at both PAX River and NTTR. Later, the UCF team was also tasked to analyze the Integrated RF/Optical Networked Tactical Targeting Networking Technologies (IRON-T2) data taken over a 147-km link between two mountains in Hawaii on October 16, 2008.

The UCF team took direct measurements of only the beacon beam at NTTR and made no measurements at PAX River or Hawaii. The beacon beam data collected by UCF was used to calculate path-averaged atmospheric parameters and to investigate aero-optic effects. In addition, UCF was provided with some of the power in the fiber (PIF) data taken by NGC on the ORCA data beam at NTTR and at PAX River in order to address the fading statistics associated with the data beam and the benefit of the AO compensation system. Some of the difficulties encountered by the UCF team during this analysis was attempting to correlate local times at which the data was taken with aircraft position and also determining the gimbal angle of the turret mounted in the nose of the aircraft. The gimbal angle as reported by the aircraft was recorded for PAX testing; however, for NTTR testing the gimbal angle was not reported and had to be inferred from the crude GPS location of the aircraft, thus rendering it less accurate. Additionally, based on discussions with NGC it was not certain whether the data given to UCF for the PAX River testing were for the uplink or downlink propagation path. It was finally concluded by UCF from data analysis that the data were for uplink propagation from ground to aircraft.

In the Introduction (Section 1) we first review results of the measured data taken over a 10-km path near ground in August 2008 at Campbell, CA and compare these results with UCF theoretical models. The data includes mean power in the bucket (PIB) and mean PIF, with and without the AO compensation system turned on. We believe this analysis helps to validate the UCF models used for NTTR data analysis and PAX River data analysis. The UCF models separately account for tip-tilt compensation alone at each end of the link and also full AO compensation at each end of the link like the ORCA system. The measured data at Campbell shows an increase in mean PIF of approximately 5-18 dB when the AO system is turned on as compared with the AO system turned off. The UCF tip-tilt model shows a maximum increase in mean PIF of roughly 4 dB when using only tip-tilt corrections at each end of the link. Hence, higher-order AO compensation can potentially increase mean PIF by up to 14 dB over tip-tilt compensation alone, at least on a 10-km path. At longer ranges, the 18 dB gain over an uncompensated AO system is probably unrealistic owing to the Rayleigh range limitation on higher-order AO compensation modes.

In Section 2 we review the path-averaged parameters measured on the downlink beacon beam during Flight #2 on May 16, 2009 (Table 2) [1]. Next, we show evidence of the aero-optic effect on the mean irradiance and variance of irradiance of this measured beacon data as the gimbal angle changes from zero to 90 deg and greater. The trend of the measured data is increasing mean irradiance and variance with increasing gimbal angle up to 90 deg and then decreasing again with even larger gimbal angles. That is, the aero-optic effect is most benign when the aircraft is flying directly toward the receiver and greatest when the aircraft is flying transverse to the propagation path. However, the aero-optic effect does not show up in the scintillation index at any gimbal angle, which is the variance divided by the square of the mean irradiance. Further evidence of the aero-optic effect is revealed by the power spectral density (PSD) of the beacon beam. By plotting the product of the frequency and the PSD, the resulting graph shows a characteristic hump around 22-30 Hz, depicting low frequency atmospheric effects independent of the orientation of the aircraft or gimbal angle. This low frequency hump shows that most of the irradiance

fluctuations are caused by larger atmospheric scale sizes. As the gimbal angle increases, a high frequency hump begins to appear between 300-700 Hz (but extending out to 1 kHz and beyond) that we attribute to the aero-optic boundary layer. This secondary hump is also present in wind tunnel data [3]. Graphs presented in Appendix A clearly show the buildup of higher frequencies forming a secondary hump as the gimbal angle increases from near zero to beyond 90 deg. We also examined the inferred probability density function (PDF) from 1 s histograms of the same data. Our conclusion was that neither the gamma-gamma PDF nor the lognormal PDF fit the PDF data very well for small values of the irradiance. We believe this is mostly a consequence of aperture averaging that was present even in our smallest 2-in aperture.

Downlink ORCA data beam measurements at NTTR provided by NGC are examined in Section 3. The data came from direct measurements of the PIF during Flights #1 and #2 on May 17. We restrict the analysis in this report to only Flight #1, however, because it is not clear that the system was working properly during Flight #2. We used the HAP C_n^2 profile model [see Eq. (3)] to develop a statistical prediction model for estimating various parameters associated with the data beam, such as Fried's parameter, Strehl ratio, PIB and PIF. In this theoretical analysis we also included a model for tip-tilt compensation at both the transmitter and receiver ends of the propagation link. However, atmospheric measurements were only made on May 16 and the NTTR data beam measurements that we examined were taken during Flight #1 on May 17. Without direct atmospheric measurements during the flight times of the data measurements, we cannot predict the beam statistical parameters with great certainty. We base our theoretical analysis on the average atmospheric conditions that were measured by the UCF team during Flight #2 on May 16. However, the Weather Research and Forecasting (WRF) Model that was used in Ref. [2] to estimate Fried's parameter during flight time measurement periods on May 17 suggests that atmospheric turbulence was stronger much of the time on May 17 than it was on May 16.

We select the HAP model with background turbulence characterized by $M = 3.3$ and ground-level refractive-index structure parameter $C_n^2(h_0) = 1.89\times10^{-13}$ m$^{-2/3}$, which represent average atmospheric conditions during May 16 measurements by UCF [1]. From this May 16 HAP model, we obtain the average Fried parameter values shown in Fig. S1 for various ranges. We note that r_0 values for the100 km range on May 16 varied over 4-20 cm with the average given below at roughly 8 cm. The May 16 model in Fig. S1 predicts larger values of Fried's parameter by roughly a factor of 2.5 compared with that from the WRF model for May 17. The WRF model also predicted smaller r_0 values for May 16 (i.e., stronger turbulence conditions) compared with values deduced from UCF measurements.

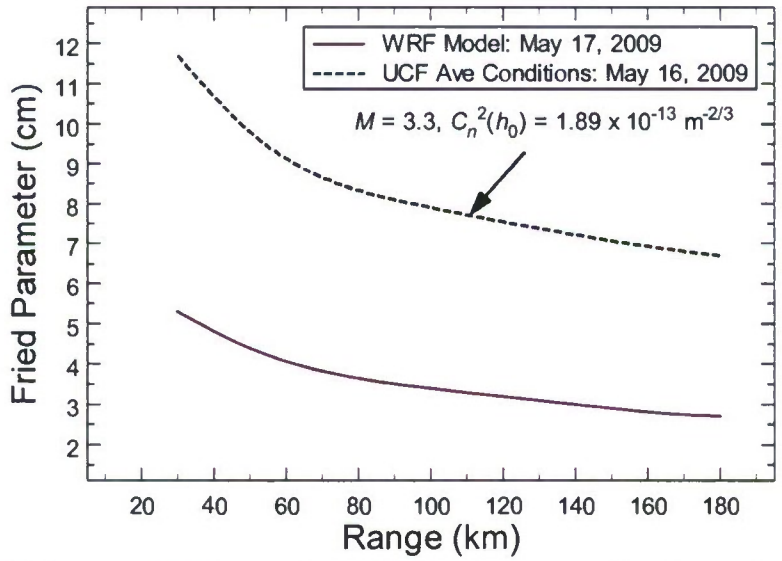

Figure S1 Fried parameter estimates from the HAP model based on May 16 atmospheric measurements by UCF (dashed line) and May 17 estimations from the Weather Research and Forecasting model (solid line).

In Fig. S2 we plot a number of 5 s data samples of the mean PIF from Flight #1 data taken by NGC at NTTR on May 17, 2009. Also shown in Fig. S2 are theoretical curves based on no AO compensation with a

gimbal angle near 90 deg (solid line) and a gimbal angle near zero (dashed blue line). The Tx power was assumed to be $P_T = 33.5$ dBm. A third theoretical curve (dotted red line) corresponding to full AO compensation using 35 Zernike modes is also featured. Based on these theoretical models, a full AO compensation system would improve the mean PIF by approximately 5-9 dB over no AO compensation system in the presence of aero-optic effects, and by 3-6 dB in the absence of aero-optic effects. The full AO compensation theoretical curve predicts mean PIF values consistent with those published in the SPIE Proceedings by Stotts et. al [2]. Most of the mean PIF values below -41 dBm are probably system level failure errors.

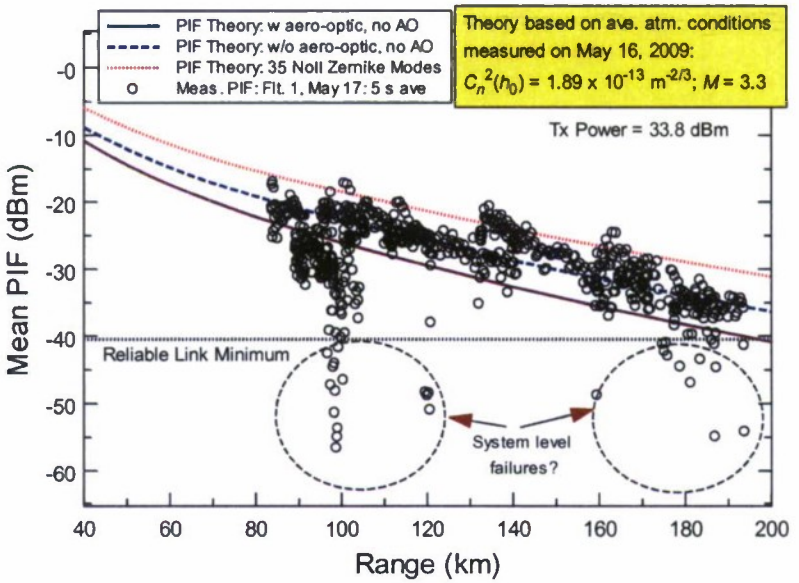

Figure S2 Mean PIF data taken during Flight #1 on May 17, 2009. The data represents measurements made over a 5 s timeframe with Tx power $P_T = 33.8$ dBm.

In addition to mean PIF values, the UCF team also calculated the mean fade time and subsequent packet loss per fade assuming a 5 Gbps data rate. The calculated mean fade times for Flight #1 on May 17 are plotted as a function of range below in Fig. S3. Mean fade times for Flight #1 were mostly shorter than 2 ms and often shorter than 1 ms. Also shown in Fig. S3 are mean packet losses per fade corresponding to the fade data for Flight #1 on May 17.

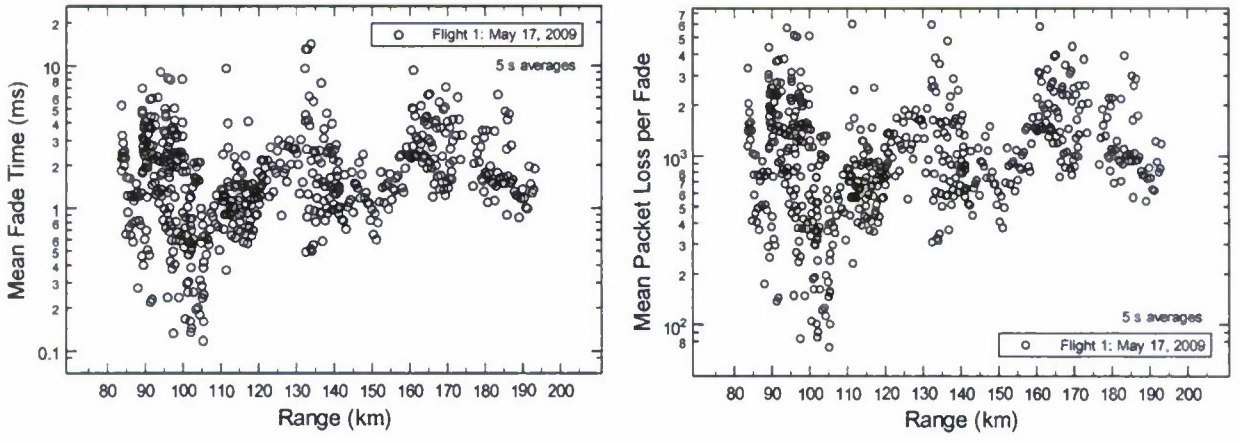

Figure S3 Mean fade time in ms and mean packet loss per fade calculated from PIF data taken during Flight #1 on May 17, 2009. The data represents mean fade measurements made over a 5 s timeframe.

The data given to UCF for the PAX River testing were taken during early morning hours on an uplink propagation path. First we examined the mean irradiance and variance of the PAX data to look for evidence of aero-optic effects. As expected for an uplink path, aero-optic effects at the aircraft were negligible. We then did theoretical predictions on the same beam parameters that were calculated for the data at NTTR. Based upon macroscale meteorological parameters at the time of the flight, we used the Kopeika model to estimate a ground-level C_n^2 value of 0.83×10^{-15} $m^{-2/3}$ and background turbulence strength of $M = 0.5$ in the HAP model. These conditions produce a Fried parameter estimate of 29 cm uplink at 70 km range, a little larger than the 23 cm predicted by the WRF model. In Fig. S4 below we plot some of the mean PIF data taken at PAX River on May 12, 2009, along with theoretical values based on transmitted power of 31.2 dBm. The blue dashed-dotted curve corresponds to the AO compensation system turned off and the red dotted curve corresponds to the full AO compensation system turned on. Although the theoretical curves provide a reasonable match to the mean PIF data at all ranges, some of the measured mean PIF values are 2-3 dB higher at shorter ranges (less than 55 km) than any theoretical values with tip-tilt compensation or even full AO compensation. We believe from these results that the full AO compensation system was likely operational at both the transmitter and receiver ends of the link at PAX River.

In addition to mean PIF values, the mean fade time, variance, and packet loss per fade was determined for the data taken at PAX River. In Fig. S5 we plot the mean fade time and mean packet loss per fade vs range for the PAX River data. All mean fade times were less than 0.2 ms.

We were also provided with data from the DARPA/ AFRL Integrated RF/Optical Networked Tactical Targeting Networking Technologies (IRON-T2) tests conducted on October 16, 2008 along a 147-km path between Haleakala and Mauna Loa in Hawaii. This data led to mean PIF values between -21 dBm to -18 dBm. The median values for this data were also calculated and found to be between -26 dBm and -23 dBm. Median values for PIF are always a few dB lower than corresponding mean PIF values. Mean fade times were typically less than 0.2 ms. Atmospheric conditions on each mountain were not available.

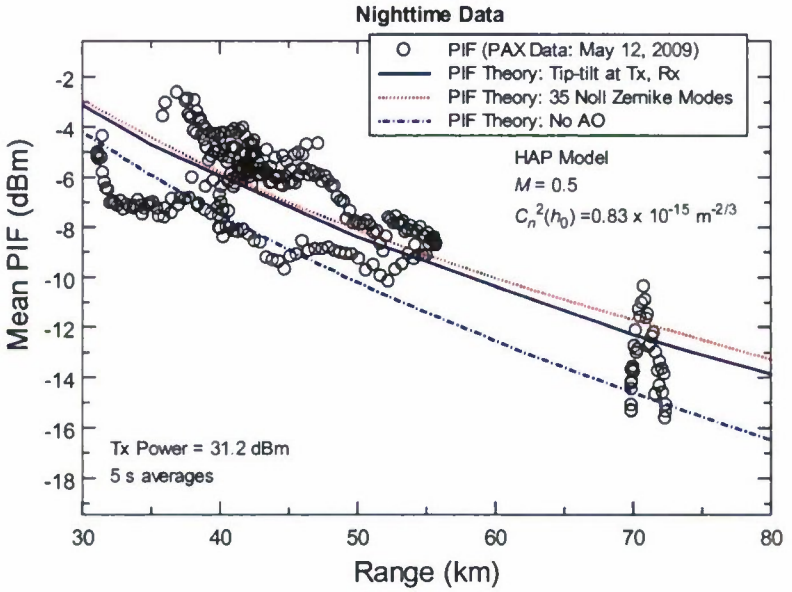

Figure S4 Mean PIF data taken during preliminary flights on May 12, 2009, at PAX River. The data represents measurements made over a 5 s timeframe.

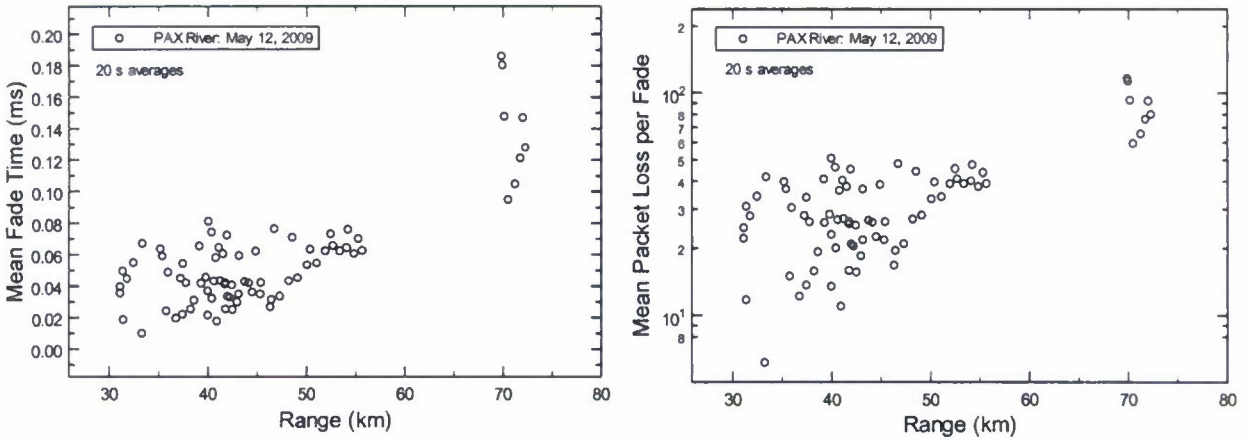

Figure S5 Mean fade time in ms and mean packet loss per fade calculated from PIF data taken during PAX River testing on May 12, 2009. The data represents mean fade measurements made over a 20 s timeframe.

To obtain a better assessment of a full AO compensation system compared with one using only tip-tilt, we also examined a horizontal path similar to that for air-to-air propagation between aircraft over ranges from 10 km up to 200 km. We assumed strong turbulence conditions with $M = 25$ in the HAP model. In Fig. S6 we show theoretical mean PIF values for no AO compensation, Tx and Rx tip-tilt only, and full AO compensation. Aero-optic effects are neglected in this analysis. Notice that a full AO compensation system can improve mean PIF by up to 12 dB over no AO at 200 km, but offers little improvement in mean PIF at 10 km. These results are different than those at Campbell because now the atmospheric turbulence (i.e., C_n^2) is very weak by comparison. The assumed transmitted power is 1.0 Watt (30 dBm).

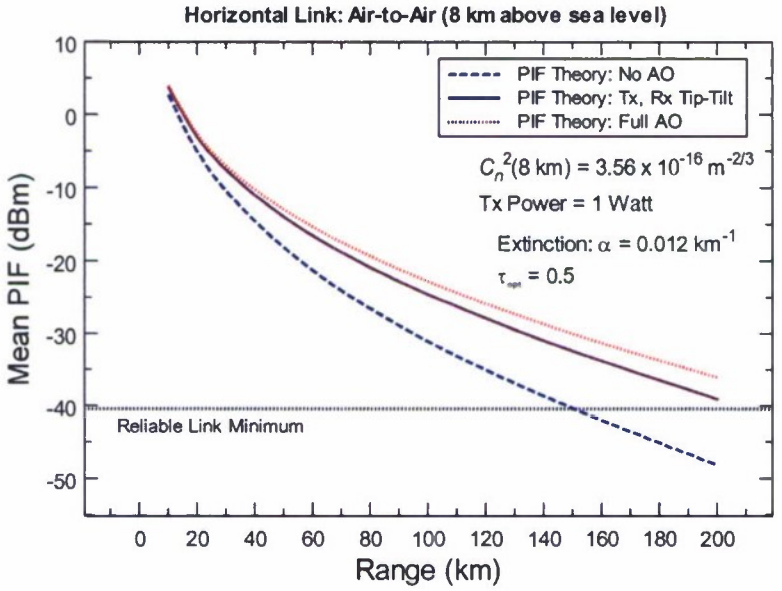

Figure S6 Theoretical prediction of mean PIF as a function of range for an air-to-air propagation path. Aero-optic effects are neglected.

The last analysis that we performed was to examine a simple predictive C_n^2 model developed by Kopeika and his colleagues [5,6], called the BKB model, that is based on measurements of macroscale parameters such as air temperature, wind speed and direction, and relative humidity, all of which do not vary too greatly with distance. In our analysis we use macroscale atmospheric parameters measured at Antelope Peak on May 16, 2009 and compare the values of C_n^2 predicted by the BKB model with scintillometer values actually measured at Antelope Peak during the same time period. We found excellent agreement between the two methods, giving credence to our claim in a previous report [1] that C_n^2 values measured near ground on a ledge below the NGC system on Antelope Peak are essentially the same that would be found near ground at the NGC test site.

Conclusions from UCF Analysis

1. *Aero-optic effects:*

Beacon data collected at NTTR show that the aero-optic boundary layer can increase the mean irradiance and variance with minimum effect for gimbal angles near zero and maximum effect with gimbal angles near 90 deg. The same is true for the PSD of the measured irradiance. However, the scintillation index is not affected by the presence of the aero-optic boundary layer.

Conclusions:

- Under *moderate level atmospheric turbulence*, the presence of aero-optic effects can reduce the mean PIF by roughly 3-6 dB at all ranges
- Under *much stronger atmospheric turbulence*, the mean PIF is reduced by only 1-2 dB

2. *Full adaptive optics compensation:*

Conclusions:

- *Tip-tilt alone* can improve mean PIF by 4-7 dB over all ORCA ranges (50 km up to 200 km)
- *Full AO compensation over short ranges* (10 km) near the ground can improve mean PIF by 5-18 dB over no AO compensation (e.g., Campbell range)
- *Full AO compensation over longer ranges* (30-70 km) at aircraft altitudes can improve mean PIF by 3-8 dB over no AO compensation
- *Full AO compensation over long ranges* (> 100 km) at aircraft altitudes can improve mean PIF by 10-12 dB over no AO compensation.

3. *Comparison between PAX River data and NTTR data:*

Conclusions: The statistics for mean PIF, mean fade time, and mean packet loss per fade are much better than those obtained at NTTR. There are several reasons why this might be true:

- Typical *ranges* at PAX River were shorter than those at NTTR.
- *Background turbulence* was probably much weaker at PAX River (nighttime testing) than at NTTR (daytime testing).
- *Aero-optic effects* were not present at PAX River because the data was taken on the uplink path.
- The *AO compensation system* appeared to be fully operational during most of the PAX River testing but perhaps not so at all NTTR testing. (This conjecture is based on theoretical analysis without the benefit of actual atmospheric measurements during testing.)
- The *propagation path* at PAX River was mostly over water whereas that at NTTR was over mountains. The difference in terrains between the two sites undoubtedly led to some of the differences in the data.

TABLE OF CONTENTS

1. INTRODUCTION

The reliability of the ORCA communication channel due to a laser beam passing through atmospheric turbulence can be deduced from analysis of the power that enters the optical fiber. Of some concern in this analysis is the effect of the aero-optic boundary layer around the aircraft that can introduce fluctuations in the beam other than those caused by atmospheric turbulence between the aircraft and the optical receiver. Although the ORCA data beam was not directly measured at the receiver except for power in the fiber (PIF), the beacon transmitted from the aircraft to a ground station on Antelope Peak was measured by a team from the University of Central Florida (UCF) that provided information about the aero-optic boundary layer as well as about the atmospheric turbulence along the optical channel [1].

In addition to PIF, other measures of reliability or performance capability of the ORCA free space optical communication (FSOC) system is the captured power in the bucket (PIB) by the receiver aperture and the fade statistics associated with the data beam. The *fractional fade time* (also called the probability of fade) describes the percentage of time the irradiance of the received wave is below some given threshold value. For the ORCA system the threshold of the mean PIF is taken at -41 dBm. Perhaps more important than knowing the probability of fade is knowing the *mean fade time*, i.e., the average length of a fade below threshold over a given time frame, and the implied packet loss per fade based on a given data rate.

In the immediate analysis below, we present data taken at Campbell, CA over a 10-km range with the ORCA adaptive optics (AO) system turned on and also turned off. This data provides a baseline for how much improvement the AO system can provide in both mean PIB and PIF without AO. We compare these statistics with those from UCF theoretical models that account for only tip-tilt compensation at both ends of the laser link or for full AO compensation. In later sections we examine data obtained from Northrop Grumman Corporation (NGC) for testing at the Nevada Test and Training Range (NTTR) located on the Nellis Air Force Base near Tonopah, NV, and that obtained during preliminary testing at Patuxent (PAX) River Naval Air Base in Maryland. Once again, we compare measured mean PIF values with those obtained from the UCF theoretical models and also with those values reported by Stotts, et. al [2]. We further examine data for evidence of aero-optic effects, particularly when the aircraft is flying transverse to the direction of propagation (gimbal angle near 90 deg) and when the aircraft is flying directly toward the receiver (gimbal angle near zero). Finally, we present some theoretical C_n^2 models for turbulence near the ground based on macroscale weather parameters such as air temperature, wind speed, and relative humidity, all of which do not vary too greatly with distance. These theoretical models are compared with C_n^2 measurements made on Antelope Peak using the macroscale weather parameters measured by the UCF team.

1.1 Campbell Measurements

Here we first want to compare our theoretical models for PIB and PIF with the 2008 DARPA/AFRL sponsored ORCA Program testing over a 10-km range at Campbell, CA. One UCF theoretical model assumes that only tip-tilt corrections are present at both transmitter (Tx) and receiver (Rx) ends of the link, whereas the second model and the measured data utilizes a full higher-order AO compensation system at both ends using Noll's results for 35 modes. It has been determined, however, that higher-order AO (beyond tip-tilt) will not resolve optical distortion beyond the Rayleigh range at either end of the link.

As presented in our September 2009 Report [1], the mean PIB is estimated from the relation

$$\mathrm{PIB} = \frac{\tau_{\mathrm{atm}} \tau_{\mathrm{opt}} P_{\mathrm{Tx}} D_{\mathrm{Rx}}^2 \, \mathrm{SR}}{8W^2}, \tag{1}$$

where $\tau_{\mathrm{atm}} = 0.6$ is the assumed transmittance of the atmosphere in the analysis of the Campbell data, $\tau_{\mathrm{opt}} = 0.6$ is the assumed transmittance of the optics, $P_{\mathrm{Tx}} = 0.025$ Watts is the assumed transmitted power, $D_{\mathrm{Rx}} = 10$ cm is the diameter of the receiver aperture, SR is the Strehl ratio, and W is the free-space Gaussian beam radius in the pupil plane of the receiver. Including the presence of other optical elements and possible spot size mismatch at the optical fiber entrance, there is also a high power optical circulator between the PIB and the PIF to separate the outgoing high power beam from the incoming signal that presents some additional losses. Thus, the mean PIF is calculated from the relation

$$\mathrm{PIF} = \tau_{\mathrm{opt}}\,\mathrm{PIB}\,f_{\mathrm{Airy}}\left(\frac{4}{\beta^2}\right)\mathrm{SR}_{\mathrm{f}}, \tag{2}$$

where SR_{f} is the Strehl ratio associated with the beam entering the fiber core and $f_{\mathrm{Airy}} \approx 0.2$ is the assumed fraction of power entering the fiber for a diffraction limited beam through the optical circulator. The spot size mismatch factor β at the fiber from Fig. 26 in the September Report [1] is also used here. The spot size mismatch at the fiber entrance leads to approximately 1-2 dB loss without AO compensation.

In Table 1(*a*) we present measured results of mean PIB and PIF obtained at Campbell using higher-order AO compensation (yellow shaded columns) as well as theoretical results from UCF models. The first UCF theoretical model uses only Tx and Rx tip-tilt compensation (green columns) whereas the second model (tan shaded columns) also includes higher-order AO corrections based on Noll's results [9] for phase improvements, i.e., $\mathrm{SR}_{35\mathrm{modes}} = 1/[1+0.014(D_{Rx}/r_0)^{5/3}]$. The dB improvement when the AO system is turned on is presented in Table 1(*b*). The C_n^2 values were inferred by Alan Pike (private communication), not measured.

Table 1(*a*) Measured results of mean PIB and PIF over a 10-km range at Campbell, CA in 2008. Modeled results by UCF include only tip-tilt at Tx and Rx and full AO compensation using Noll's results for 35 modes.

Time/ Date	C_n^2 x 10^{14}	Tx/Rx AO Status	Meas. PIB (dBm)	Meas. PIF (dBm)	Modeled UCF-PIB (dBm)	Modeled UCF-PIF (dBm)	Modeled UCF-PIB (dBm)	Modeled UCF-PIF (dBm)
9 AM	1.25	On	-3.5	-15.4	-7.9	-23.1	-7.9	-18.8
8/27/08	1.25	Off	-11.2	-33.8	-11.6	-33.8	-11.6	-33.8
1 PM	0.89	On	-4.2	-17.0	-6.9	-20.8	-6.9	-17.3
8/27/08	0.89	Off	-10.0	-30.1	-10.3	-30.4	-10.3	-30.4
2 PM	1.10	On	-4.2	-16.9	-7.5	-22.2	-7.5	-18.2
27/08	1.10	Off	-10.0	-32.1	-11.1	-32.5	-11.1	-32.5
6 PM	0.205	On	-6.0	-13.4	-4.1	-14.6	-4.1	-13.5
8/27/08	0.205	Off	-5.2	-17.9	-5.9	-19.0	-5.9	-19.0
					Tip-Tilt Only		Full AO: 35 Modes Noll	

Table 1(*b*) AO improvement results of mean PIB and PIF from Table 1(*a*).

Time	AO Improve. Meas. PIB	AO Improve. Meas. PIF	AO Improve. UCF-PIB	AO Improve. UCF-PIF	AO Improve. UCF-PIB	AO Improve. UCF-PIF
9 AM	7.7 dB	18.4 dB	3.7 dB	10.7 dB	3.7 dB	15.0 dB
1 PM	5.8 dB	13.1 dB	3.4 dB	9.6 dB	3.4 dB	13.1 dB
2 PM	5.8 dB	15.2 dB	3.6 dB	10.3 dB	3.6 dB	14.3 dB
6 PM	----	4.5 dB	1.8 dB	4.4 dB	1.8 dB	5.5 dB
			Tip-Tilt Only		Full AO: 35 Modes Noll	

The theoretical PIB and PIF by UCF is generally within 1 dB of measured results with AO compensation off, and also within 1-4 dB of measured results with full AO compensation on. Although the results are only for a single short range, we believe the closeness of the results with measured data provides some validation of the UCF theoretical PIB and PIF models. The AO-on tip-tilt only compensation by UCF analysis shows PIB improvements of approximately 2-4 dB and PIF improvements of approximately 6-15 dB compared with AO compensation off. However, the measured PIB and PIF with full AO-on gave improvements of 6-8 dB and 5-18 dB, respectively.

Over longer ranges up to 200 km the same improvement in mean PIB and PIF may not always be realized from higher-order AO compensation beyond tip-tilt. In part, this is because the Rayleigh range higher-order AO limitation is only for roughly 4.5 km at each end of the link—a rather small percentage of the total path length for these much longer paths. Also, long propagation paths will be at aircraft altitudes where the atmospheric turbulence is much weaker than near the ground.

2. NTTR DATA ANALYSIS: BEACON BEAM

During May 16-18, 2009 measurements were made on the ORCA laser beam (1550 nm) transmitted from/to a BAC 1-11 aircraft to/from the top of Antelope Peak located at NTTR. The ORCA data beam was transmitted from a 10-cm aperture and received by a 10-cm aperture in both directions. A parallel test was conducted by a University of Central Florida (UCF) team using the laser beacon from the BAC 1-11 aircraft operating at 878 nm from a 2.54-cm transmitter aperture with a full-angle beam divergence of 6000 microradians. The small aperture and large divergence angle led to a ground footprint of 300-1200m for ranges of 50-200 km, respectively. The large footprint on the ground ensured that the UCF testing equipment would always be near the center of the beacon beam even though the equipment location was several meters from the NGC testing equipment. The purpose of the UCF testing was to characterize the atmospheric channel between the aircraft and Antelope Peak by determining path-averaged values of the refractive-index structure parameter C_n^2, the inner scale of turbulence l_0, and the outer scale of turbulence L_0. In a previous report (September 2009) we described the operation performed by the UCF-CSC group to support the NGC testing of the ORCA system and the atmospheric channel data collected by the UCF team at NTTR [1]. In that report we also described how the path-averaged values of atmospheric parameters calculated from the measurements were used to develop a C_n^2 profile model as a function of altitude. This C_n^2 profile model is a small modification of the near-ground term of the Hufnagel-Valley model suggested by Valley to allow the original Hufnagel model to extend from the 3-km floor down to the ground. The new model is called the HAP model and uses the tested fact [12] that C_n^2 values near the ground are best described by a -4/3 power law during daytime hours and a -2/3 power law during evening hours.

2.1 Beacon Data From UCF Team: Path-Averaged Atmospheric Parameters

In this section we will briefly review the measurements made by the UCF team at Antelope Peak during Flight #2 on May 16, 2009. A tracking mount holding six telescopes was used to track and record irradiance data from the laser beacon on the NGC BAC 1-11 airplane. The airplane was manually acquired and tracked using three tracking telescopes. The three tracking telescopes had different field-of-views and recorded video of the airplane and beacon. In addition to the three tracking telescopes, three uniquely sized (effective) aperture telescopes (D_j, j = 1,2,3) were used to simultaneously record the laser irradiance from the airplane's beacon. The normalized variance of irradiance, or scintillation index (SI), was calculated for each of the three telescopes. Large apertures produce lower SI values so each telescope produced a different SI. A minimization problem was set up for the magnitude-squared difference between scintillation theory, $\sigma_I^2\left(l_0, L_0, C_n^2, D_j\right)$, and the experimental aperture-averaged SI values, $\sigma_{I,\exp}^2\left(D_j\right)$. Solving the minimization problem resulted in the path-averaged atmospheric parameters, C_n^2, l_0, and L_0, encountered by the ORCA beacon link. The location of the equipment on Antelope Peak is shown in the aerial view in Fig. 1. The ground level scintillometer instruments and weather station were positioned on a ledge below the plateau on which the NGC system and the UCF-CSC tracking mount were located. Figure 2 is a diagram showing the general setup for the weather instrumentation and scintillometers.

Figure 1 Aerial view of Antelope Peak illustrating placement of the test equipment.

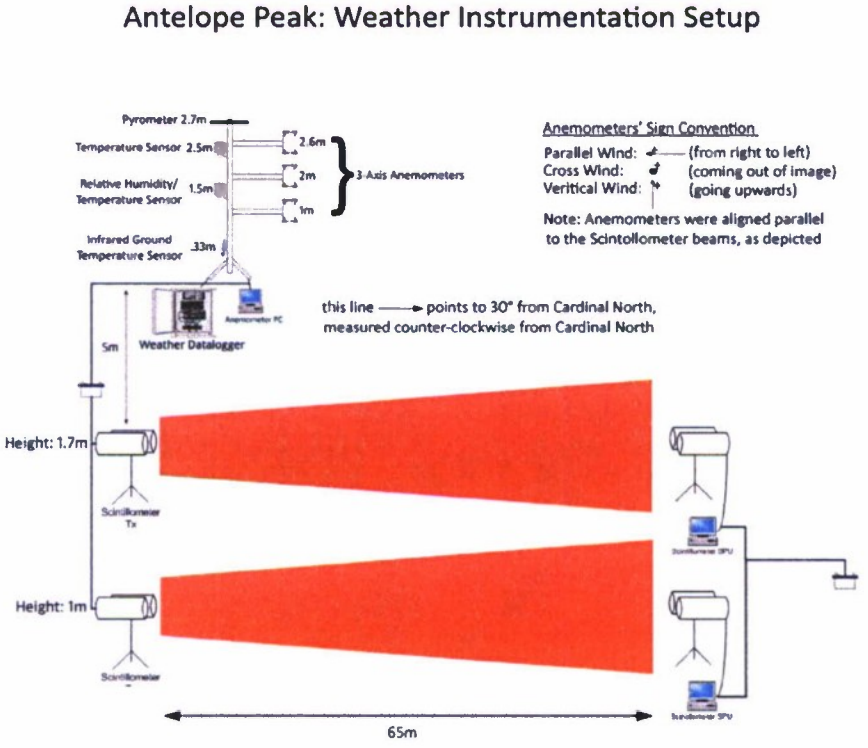

Figure 2 Schematic of the weather station setup on Antelope Peak.

In our previous September 2009 report [1] we presented path-averaged values of the three atmospheric parameters: C_n^2, l_0, and L_0. Most of the UCF data was obtained during Flight #2 on May 16, 2009. Path-averaged values for Flight #2 are shown below in Table 2. The three telescope diameters used at Antelope Peak were D_1 = 2 in (5.1 cm), D_2 = 5.4 in (13.7 cm), and D_3 = 10.7 in (27.2 cm), the smaller aperture diameters obtained by placing variable sized irises in front of two 6-in telescopes. The 11-in telescope had no iris but was a Cassegrain model with a 2-in obscuration, so the effective diameter (based on collecting area) was approximately 10.7 in. The detectors used to record the laser irradiance were dc coupled avalanche photodiodes (APD). As long as the beacon was on, data were being recorded. The data were recorded simultaneously from the APDs at a rate of 10 kHz. Periodically, the dc sky background was measured by moving the collecting telescopes away from the beacon beam.

In analyzing the data for computing path-averaged values, we first restricted the analysis to stationary data segments for which the mean irradiance and variance were almost constant (typically only 15-40 s in length). This treatment of the data provided only a small number of path-averaged values. Hence, upon further analysis of the Flight #2, May 16 data sets over 20 s time segments, including times when the mean and variance were changing, we found some data sets where the path-averaged C_n^2 values were 4 to 10 times larger than those based on stationary increments. The reason for the occasional increase in path-averaged C_n^2 is not clear at this time. However, it may be a consequence of the beam sometimes passing closely above high mountain peaks between Antelope Peak and the aircraft, resulting in strong turbulence conditions over a portion of the path (like a thick phase screen) caused by the strong updrafts above the peaks. In analyzing the scintillation data used to determine the path-averaged atmospheric parameters, we did not detect evidence that the aero-optic boundary layer around the aircraft had any effect on the calculated scintillation index from direct measurements. In particular, the entries in Table 1 marked 'Head On' should be virtually independent of aero-optic effects, i.e., the scintillation index values are comparable with those in the table where the aircraft was flying at some gimbal angel other than zero. See Sections 2.2 and 2.3 for more discussion about aero-optic effects.

It should be pointed out that path-averaged C_n^2 values obtained by these measurements are nonlinearly-weighted averages through calculation of the scintillation index. This means that values near the transmitter or receiver contribute less to the path-average C_n^2 than values elsewhere along the path. This is in contrast with Fried's parameter r_0 that depends more on C_n^2 values near the receiver. Calculating Fried's parameter r_0, and other statistical quantities that are primarily related to phase fluctuations near the receiver, will lead to only rough estimates of their actual values when using path-averaged C_n^2 values. Also, path-averaged values found on a downlink path do not apply for an uplink path (i.e., the paths are non-reciprocal). Nonetheless, the downlink path-averaged values can be useful in describing the scintillation index of the data beam, the fade statistics (probability of fade and mean fade time) and also for describing the bit-error-rate (BER) of the data beam on the downlink path.

Table 2 Scintillation data measured from aircraft beacon during Flight #2 on May 16, 2009. The numbers in parentheses are the calculated theoretical scintillation values based on path-averaged atmospheric parameters. Flight times where the aircraft is flying directly toward the receiver are marked "**Head on**." It is believed that the lavender shaded path-average C_n^2 values correspond to instances where large updrafts from high mountains exist along the propagation path.

Start Time-PST (Duration)	*Range*	*Scin Index 1* Rx=5.1cm	*Scin Index 2* Rx=13.7cm	*Scin Index 3* Rx=27.2cm	*Path Ave* C_n^2 ($m^{-2/3}$)	*Path Ave Inner Scale*	*Path Ave Outer Scale*
Flight 2	**May 16, 2009**	*Theory in Parens*	*Theory in Parens*	*Theory in Parens*			
~17:27 (----)	97 km	0.89 (0.89)	0.58 (0.59)	0.33 (0.30)	2.33×10^{-17}	0.43 cm	2.7 m
17:27:42 (60 s)	95 km	0.90 (0.91)	0.35 (0.43)	0.34 (0.30)	2.15×10^{-16}	0.71 cm	4.08 m
17:30:07 (21 s)	95 km	1.60 (1.60)	1.36 (1.01)	0.41 (0.50)	4.20×10^{-17}	1.80 cm	16.1 m
17:29:59 (60 s)	95 km	1.06 (1.08)	0.44 (0.54)	0.35 (0.35)	1.63×10^{-16}	0.72 cm	4.42 m
17:30:28 (20 s)	95 km **Head on**	1.01 (1.00)	0.55 (0.55)	0.44 (0.26)	5.44×10^{-17}	0.63 cm	2.00 m
17:30:47 (20 s)	95 km **Head on**	1.43 (1.62)	0.91 (0.91)	0.61 (0.61)	1.36×10^{-16}	1.29 cm	17.6 m
17:31:07 (20 s)	95 km **Head on**	1.37 (1.35)	0.94 (0.92)	0.48 (0.45)	2.4×10^{-17}	2.31 cm	14.2 m
17:31:27 (20 s)	95 km	1.24 (1.21)	1.04 (0.84)	0.31 (0.42)	2.0×10^{-17}	2.50 cm	10.11 m
17:31:46 (20 s)	95 km	1.24 (1.25)	1.19 (0.86)	0.32 (0.43)	2.1×10^{-17}	2.50 cm	8.24 m
17:32:06 (20 s)	95 km	1.29 (1.30)	1.29 (0.88)	0.38 (0.44)	2.5×10^{-17}	1.83 cm	9.78 m
17:32:25 (20 s)	95 km	1.02 (1.00)	0.91 (0.70)	0.29 (0.36)	2.0×10^{-17}	1.05 cm	8.07 m
17:32:45 (20 s)	95 km	0.84 (0.82)	0.70 (0.59)	0.25 (0.30)	1.37×10^{-17}	1.50 cm	5.54 m
17:33:04 (----)	95 km	0.90 (0.91)	0.72 (0.65)	0.28 (0.33)	1.42×10^{-17}	2.10 cm	9.93
17:33:24 (20 s)	95 km	1.06 (1.04)	0.79 (0.73)	0.31 (0.37)	1.70×10^{-17}	2.10 cm	8.78 m
~17:34 (----)	94 km	1.71 (1.71)	1.23 (1.23)	1.01 (1.06)	5.40×10^{-16}	4.0 cm	30.0 m
17:34:53 (39)	100 km	1.23 (1.33)	0.92 (0.90)	0.36 (0.44)	1.57×10^{-17}	1.50 cm	6.75 m
17:53:08 (20)	90 km	1.12 (1.11)	0.68 (0.70)	0.39 (0.36)	3.85×10^{-17}	0.52 cm	4.87 m
~17:55 (25 s)	94 km	1.36 (1.28)	1.25 (0.91)	0.46 (0.46)	1.68×10^{-17}	3.56 cm	20.9 m

2.2 Evidence of Aero-Optic Effect on Downlink Beacon

Some of the measured mean irradiance and irradiance variance associated with the 2-in receiver aperture and beacon laser during Flight #2 on May 16 are shown in Fig. 3 as a function of gimbal angle. The figure on the left depicts the mean irradiance and the figure on the right shows the irradiance variance, both with the same increasing behavior with increasing gimbal angle up to 90 deg. The solid curve in each figure is a "smooth average" to help visualize the behavior of the data as a function of gimbal angle. During the time period of the data in Fig. 3, no gain changes took place in the APDs—hence, the changing behavior is due entirely to the orientation (i.e., gimbal angle) of the modified MX-15 Wescam turret on the nose of the aircraft. Accordingly, we believe the behavior illustrated in Fig. 3 is a consequence of the aero-optic boundary layer which reaches its maximum effect when the plane is transverse to the propagation axis (gimbal angle of 90 deg). The scintillation index (normalized irradiance variance) formed from the ratio of the variance and square of the mean irradiance in Fig. 3 is shown in Fig. 4. Notice that, unlike the mean and variance, the solid curve in Fig. 4 formed by the ratio of the variance irradiance solid curve in Fig. 3 and square of mean irradiance solid curve in Fig. 3 appears to be independent of gimbal angle even though the mean irradiance and irradiance variance both increase with gimbal angle until around 90 deg and then decrease again.

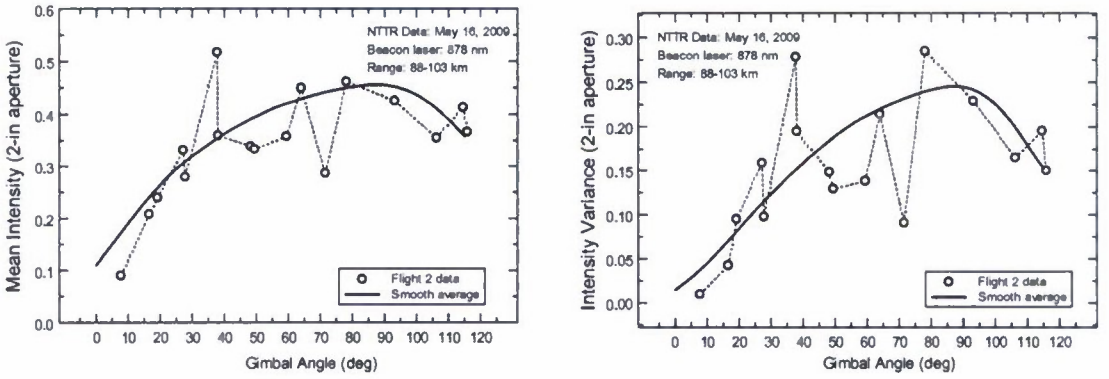

Figure 3 Mean irradiance and irradiance variance as a function of increasing gimbal angle.

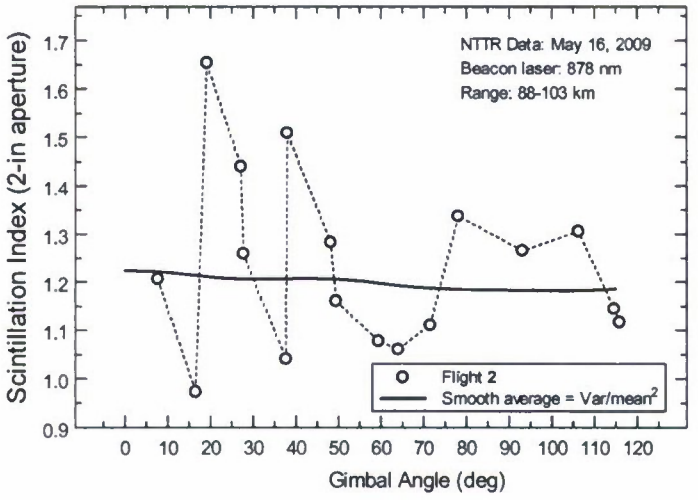

Figure 4 Scintillation index (flux variance) as a function of increasing gimbal angle.

2.3 PSD of Irradiance of Beacon Beam

The irradiance signals received at the UCF tracking mount are divided into sets of 10,000 data points. This represents one sampling period of each detector (one second of sampled data). Power spectral density (PSD) plots were created for each of the three intensity signals, utilizing a Welch spectrum estimator as the numerical method. These plots are normalized by the maximum value, such that the peak value of the curve is unity before multiplying by the frequency f.

PSD plots from data collected with the 2-in aperture during Flight #2 on May 16, 2009 were created by plotting $fS(f)$ as a function of $\log_{10}(f)$, where $S(f)$ is the PSD. By plotting the data in this fashion we can determine which frequencies contain the most power for the variance. Below in Fig. 5 we show two PSD plots of this nature—the one on the left corresponds to a gimbal angle 4 deg (aircraft is nearly head-on) and the one on the right corresponds to a gimbal angle of 85 deg (when the aircraft presents a side view). The secondary "hump" in the PSD at higher frequencies for the plot on the right can be attributed to fluctuations in the signal caused by the aero-optic boundary layer around the aircraft. We produced numerous graphs of this nature over the time period of Flight #2 on May 16. Once again, these plots clearly suggest that the aero-optic boundary layer causes additional signal fluctuations over those from the atmosphere alone. A sequence of such plots is presented in the Appendix as a function of changing gimbal angle from 46 deg to 116 deg. The low frequency hump stays centered around 22-30 Hz regardless of gimbal angle and the buildup of the high frequency hump between 300 Hz and 700 Hz can be clearly seen in this sequence of images as the gimbal angle increases. The high frequency hump also showed up in recent wind tunnel tests [3].

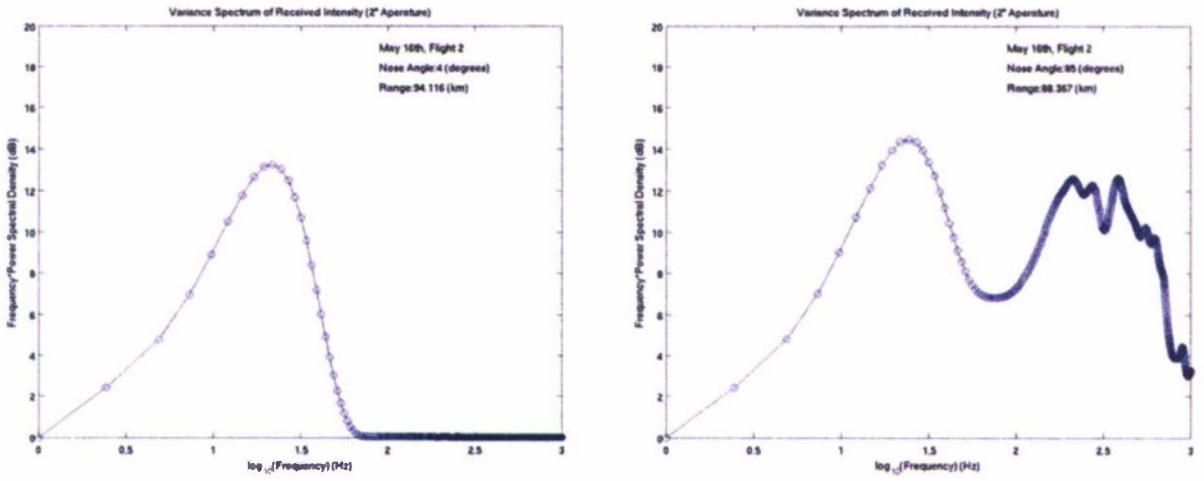

Figure 5 Plot of $fS(f)$ as a function of $\log_{10}(f)$. On the left is the PSD when the gimbal angle is near zero and on the right is the PSD when the gimbal angle is near 90 deg.

2.4 PDF and CDF of Irradiance of Beacon Beam

Knowing the theoretical form of the probability density function (PDF) is important for theoretical calculations involving fade statistics. The two theoretical models commonly used are the lognormal PDF and gamma-gamma PDF. Here we examine the data from the 2-in Rx aperture to see if either of these PDF models agrees with the data.

Because the irradiance signals are divided into sets of 10,000 data points, this represents one sampling period of the detector (one second of sampled data). The mean and variance of the irradiance signal are computed within these intervals, and thus reported once per second. The data values within each set are normalized by the mean irradiance so the mean always occurs at 0 dB. Additionally, the scintillation index

is also computed. Aircraft range and latitude/longitude (used to compute nose-angle) are reported every 10 seconds by navigation.

Histograms of the irradiance received by the telescopes were also computed over 1 second of data. The data values are shifted such that the minimum value is zero and then normalized (divided) by the mean of the data set. This allows for the histogram of the irradiance signal to be shown in decibels with respect to the mean irradiance. From the histograms, the probability distribution and the cumulative distribution are computed and the plots shown as a function of irradiance in decibels.

In Fig. 6(*a*) we plot the PDF of the irradiance signal received in the 2-in telescope during Flight #2 on May 16, 2009. In Fig. 6(*b*) we show the corresponding cumulative distritution (CDF). For the graph on the left in each figure, the gimbal angle is near zero at range 94 km with path-average atmospheric conditions described by $C_n^2 = 2.87\times10^{-17}$ m$^{-2/3}$, $l_0 = 0.57$ cm, and $L_0 = 1.97$ m. The gimbal angle is near 90 deg on the right at range 88 km and the path-average atmospheric conditions are described by $C_n^2 = 2.33\times10^{-17}$ m$^{-2/3}$, $l_0 = 1.53$ cm, and $L_0 = 8.12$ m. Also shown in the graphs in Fig. 6(*a*) are theoretical PDFs associated with the gamma-gamma distribution (solid curve) and lognormal distribution (dashed curve). Neither theoretical model fits all the data on the left side of the peak very well although the lognormal model comes closer with the PDF on the right. Both theoretical models provide a good fit to the data on the right-hand side of the peak. It has previously been shown that, whereas the gamma-gamma PDF does well for very small Rx apertures, this model doesn't always fit aperture-averaged irradiance data very well [4].

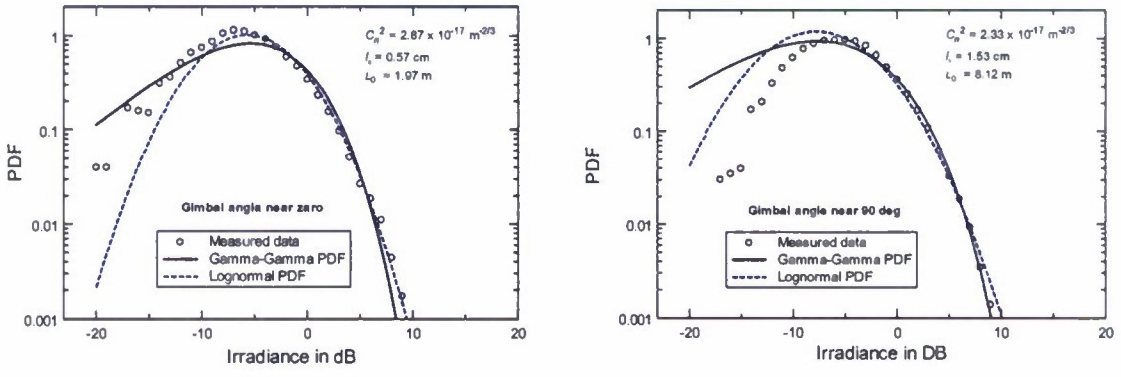

(*a*)

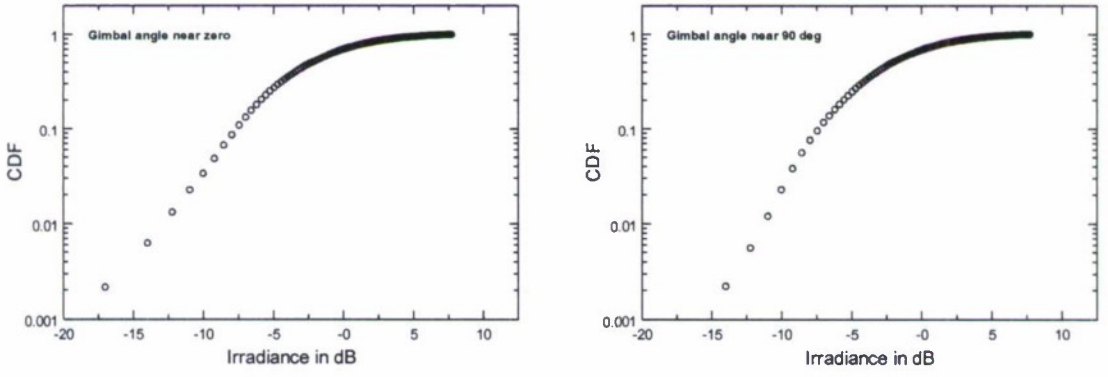

(*b*)

Figure 6 PDF (*a*) and CDF (*b*) for irradiance signal in the 2-in telescope during Flight #2 on May 16, 2009.

3. NTTR DATA ANALYSIS: DOWNLINK DATA BEAM

The data beam for the ORCA free-space optical communication (FSOC) system operates at 1.55 microns out of a 10-cm aperture. The receiver aperture is also 10 cm. In the analysis below we concentrate on the downlink data beam from the aircraft at 8016 m (26,300 ft) above sea level to Antelope Peak at 2289 m above sea level. Although the FSOC system operates in both directions, we only examined the downlink data. Of particular importance in our analysis is the determination of power in the bucket (PIB), power in the fiber (PIF), and the associated fade statistics. PIB refers to the laser light that is actually captured by the receiver aperture and PIF refers to how much of that laser light gets into the optical fiber.

3.1 Tip-Tilt Compensation for ORCA Data Beam

Both atmospheric turbulence along the propagation path and the aero-optic boundary layer around the aircraft can lead to significant losses in PIB and PIF as well as signal dropouts caused by deep fading of the optical signal. The effect of the aero-optic boundary layer around a moving aircraft has been modeled by a thin random phase screen in the UCF analysis of NTTR data taken in May 2009. Although our analysis and data suggest that such a phase screen causes no additional fluctuations in the scintillation index, it does cause additional beam spreading at the Rx through "beam wander" (i.e., a random tilt angle) on the outgoing beam from the aircraft Tx. By invoking the principle of reciprocity [5], the associated beam wander at the Rx due to the atmosphere and aero-optic boundary layer can be modeled as a random phase tilt at the Tx. By removing this random tilt at the Tx, called tracking the beam, most of the beam wander effects from the atmosphere and aero-optic phase screen can be removed. However, in the absence of aero-optic effects, such as when the gimbal angle of the aircraft is nearly zero, there is negligible beam wander on the downlink beam and hence, no random phase tilt at the Tx. That is, the atmosphere alone causes little to no beam wander on a downlink propagating beam.

In addition to beam wander, the beam may also experience another random tilt known as angle-of-arrival (AOA) fluctuations at the Rx pupil plane. This AOA tilt will manifest itself as a larger (long-term) beam spot size at the entrance to the optical fiber that can result in a loss of available PIF. By incorporating a tip-tilt correction at the Rx, the resulting spot size at the fiber will be reduced to a "short-term" spot size close to the free space spot size and consequently lead to a larger PIF value. Consequently, our theoretical analysis of the downlink beam will generally involve two components of tip-tilt—that at the Tx due to beam wander and that at the Rx due to AOA fluctuations.

Atmospheric effects will be described by the C_n^2 profile model defined by [1]

$$C_n^2(h) = M\left[0.00594\left(\frac{w}{27}\right)^2\left(\frac{h+h_s}{10^5}\right)^{10}\exp\left(-\frac{h+h_s}{1000}\right) + 2.7\times10^{-16}\exp\left(-\frac{h+h_s}{1500}\right)\right] + C_n^2(h_0)\left(\frac{h_0}{h}\right)^{4/3}, \quad h > h_0, \tag{3}$$

where h denotes height above ground, h_s represents a reference height of the ground level above sea level, and h_0 is the height of the instrumentation above ground where $C_n^2(h_0)$ is either measured or determined. In addition, we have introduced a background turbulence constant or scaling factor M that can be adjusted to fit the measured conditions at various locations. We refer to (3) as the Hufnagel/Andrews/Phillips (HAP) model. For testing at Antelope peak we set $h_s = 2289$ m and $h_0 = 2.8$ m.

No usable FSOC data was actually acquired by NGC on May 16, 2009 when UCF made atmospheric measurements due to a software problem with the ORCA system. However, data was taken by NGC from the ORCA data beam during flights on May 17, 2009 and on May 18, 2009. Our analysis below is only for Flight #1 that occurred on May 17. Although UCF did not record any atmospheric conditions at the request of the contractor on May 17, it is believed that the atmospheric conditions were similar to those on May 16. Based on May 16 measurements during Flight #2 (see Fig. 7), the average background turbulence for the HAP C_n^2 profile model was $M = 3.3$ and the average C_n^2 value at $h_0 = 2.8$ m above ground was

$C_n^2(h_0) = 1.89 \times 10^{-13}$ m$^{-2/3}$. This average C_n^2 value and background turbulence value M are used to produce the theoretical beam statistics presented in Tables 3-4 below.

Estimates for r_0 are presented in Fig. 7 of Ref. [2] for May 16 and 17 (and reproduced below in Fig. 8). However, estimates of r_0 presented in [2] are based on a Weather Research and Forecasting (WRF) model, not direct measurements. Moreover, these results are based on course measurements of atmospheric conditions over 1-km^3 regions. Note that these WRF results suggest stronger conditions of turbulence on May 16 and 17 than indicated by our measurements during Flight #2 on May 16.

NTTR: Cn2 Measurements made by UCF on May 16, 2009
Based on May 16 measurements: Flight #1 (5:30-6:00 PM)

Range (km)	Cn2(ho)	M	ro (cm)	D/ro
97	8.24E-14	0.73	13.9	0.73
95	5.00E-13	9.39	4.45	2.3
95	1.29E-13	1.57	10.5	0.97
95	3.50E-13	7.42	5.42	1.87
95	3.00E-13	0.97	6.75	1.5
95	4.20E-13	5.12	5.16	1.97
95	1.30E-13	0.47	11.1	0.91
95	9.00E-14	0.55	13.6	0.75
95	1.00E-13	0.54	12.8	0.79
95	1.26E-13	0.55	11.3	0.9
95	8.50E-14	0.55	14	0.72
95	3.50E-14	0.59	22.2	0.46
95	3.50E-14	0.61	22.1	0.46
95	3.80E-14	0.76	20.7	0.49
94	8.00E-13	26.6	3.08	3.3
100	4.00E-14	0.65	20.3	0.5
90	1.00E-13	1.61	12.1	0.84
94	4.20E-14	0.74	19.9	0.51

Average values over Flight #1

95	1.8902E-13	3.301

Figure 7 Implied C_n^2 values at 2.8 m above the ground at Antelope Peak on May 16, 2007. The parameter M represents the background turbulence level in the HAP model. The average C_n^2 value over the measurement period and average background turbulence are given at the bottom of the table.

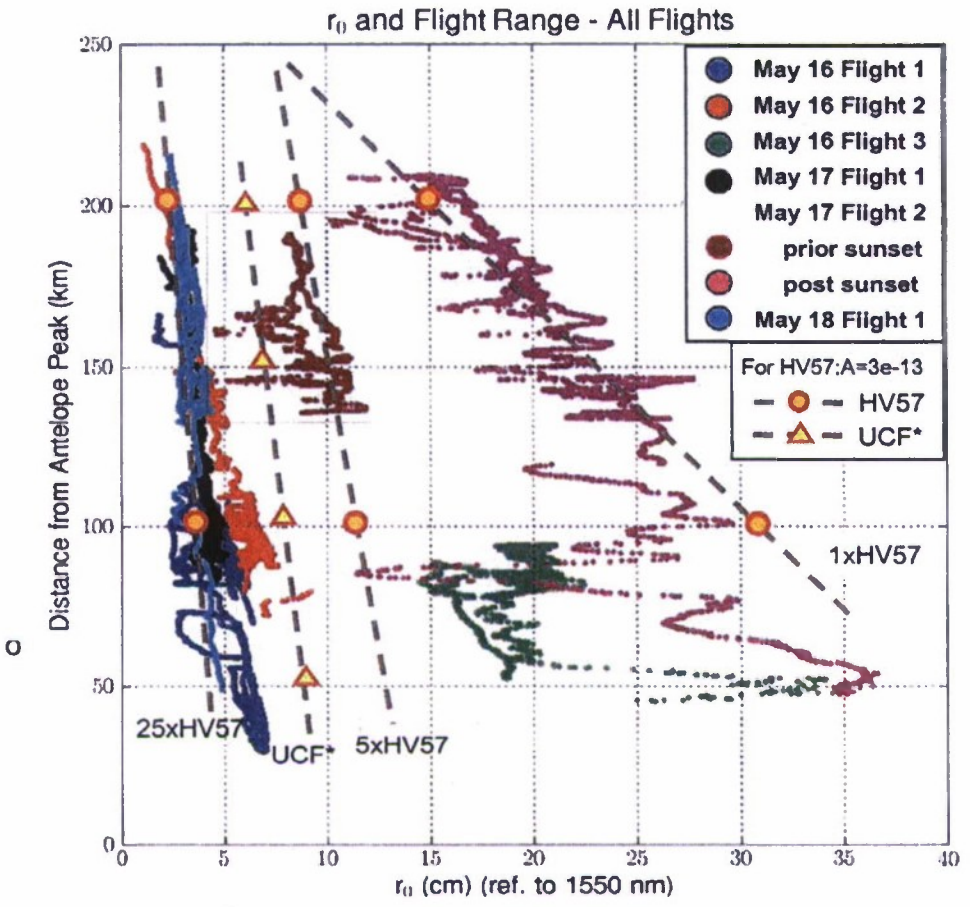

Figure 8 Fried parameter predictions based on the Weather Research and Forecasting (WRF) model plotted vs the aircraft range from Antelope Peak (taken from Ref. [2]).

The modeling that was used at NTTR is described in the September Report [1]. Basically, it relies on measured path-averaged atmospheric parameters and measurements made at ground level to determine the values of the parameter M and ground level $C_n^2(h_0)$ to be used in (3). In Tables 3 and 4 below we consider two particular measurement sets of conditions. The results in Table 3 are without aero-optic effects, which arise when the gimbal angle from the aircraft is near zero. In Table 4 we include aero-optic effects, which applies when the gimbal angle is near 90 deg. In each table we list the theoretical estimates of Fried's parameter r_0, Strehl ratio (SR), power in the bucket (PIB), and power in the fiber (PIF). The first row in Table 3 at a particular range assumes no AO compensation at the Tx or at the Rx. The second row includes both Tx and Rx tip-tilt corrections. Because beam wander effects are negligible for the downlink path in the absence of aero-optic effects and beam spreading due to atmospheric turbulence is small, the Tx tip-tilt correction alone provides only a modest improvement (less than 1 dB). The third row is based on a full AO compensation model using Noll's results [9] for reducing phase fluctuations up to 35 modes. In Table 4 we include an extra row for Tx tip-tilt alone which causes an improvement by compensating for the beam wander that arises from aero-optic effects. In the presence of aero-optic effects, we observe a drop of 2-6 dB in the theoretical mean PIF without AO compensation. Full AO compensation, or even just tip-tilt at both Tx and Rx, can remove virtually all the aero-optic effects.

The formulas used for calculating PIB and PIF with and without tip-tilt given below are based on a horizontal path for which the refractive index structure parameter is essentially constant:

Power in Bucket (No AO compensation)

τ_{opt} = transmittance of optics

τ_{atm} = transmittance of atmosphere

Power received at Rx (PIB):

$$\text{PIB} = P_{Tx} \cdot \tau_{opt} \cdot \tau_{atm} \cdot \frac{D_{Rx}^2}{8W^2} \cdot SR$$

Power in Fiber (No AO Compensation)

$f_{Airy} = 0.2$ (circulator loss)

$W_{core} = 4$ microns (fiber core radius)

Mismatch factor in spot size at fiber:

$$\beta = (W_{IP,turb} / W_{core}) + (W_{core} / W_{IP,turb})$$

Power in Fiber (PIF):

$$\text{PIF} = \text{PIB} \cdot \tau_{opt} \cdot f_{Airy} \cdot \text{SR} \cdot \frac{4}{\beta^2}$$

Power in Bucket (With Tip-Tilt)

Beam wander: $r_c^2 = 2.42 C_n^2 L^3 / W_0^{1/3}$

Short-term beam radius at Rx: $W_{ST} = \left[W_{LT}^2 - r_c^2 \right]^{1/2}$

Power in Bucket with Tx Tip - Tilt:

$$\text{PIB}_{\text{TT}} = P_{Tx} \cdot \tau_{opt} \cdot \tau_{atm} \cdot \frac{D_{Rx}^2}{8W_{ST}^2}$$

Power in Fiber (With Tip-Tilt @ Tx, Rx)

$$SR_{TT} = \frac{1}{1 + 0.28(D_{Rx} / r_0)^{5/3}};$$

$$W_{IP,turb,TT} = W_{IP} \left[1 + 0.28(D_{Rx} / r_0)^{5/3} \right]^{1/2}$$

$$\beta_{TT} = (W_{IP,turb,TT} / W_{core}) + (W_{core} / W_{IP,turb,TT})$$

Power in Fiber With Tx & Rx Tip - Tilt:

$$\text{PIF}_{\text{TT}} = \text{PIB}_{\text{TT}} \cdot \tau_{opt} \cdot f_{Airy} \cdot SR_{TT} \cdot \frac{4}{\beta_{TT}^2}$$

The free-space spot radius of the beam W_{IP} in the image plane of the receiver (incident on the optical fiber) is calculated by $W_{IP} = 2^{5/2} F / (kD_{Rx})$, where F is the focal length of the receiver lens. Of course, the above formulas for PIB and PIF must be altered for the NTTR theoretical analysis to account for the slant path between the aircraft and Antelope Peak, taking into consideration the variation in C_n^2 along the path.

The analysis in Tables 3 and 4 also includes transmittance losses caused by the atmosphere, transmittance losses through the optics, and losses due to the optical circulator as shown above. However, these are only reasonable guesses, again not based on actual measurements. We believe, however, that the relative changes in PIB and PIF shown in the tables for cases with and without tip-tilt or full AO compensation, and with and without the aero-optic consequence, may reasonably reflect actual changes in how the system works.

In arriving at our results in the tables, we assumed that atmospheric extinction was $\alpha = 0.012$ km^{-1} with transmittance $\tau_{\text{atm}} = e^{-\alpha L}$, where L is range in km; the optics transmittance was $\tau_{\text{opt}} = 0.5$; and the transmitted power was $P_{\text{Tx}} = 33.8$ dBm. Spot size mismatch causes 1-2 dB loss in mean PIF without AO compensation, but virtually no loss with full AO compensation.

Following our theoretical analysis of the NTTR test data under moderate-to-strong atmospheric conditions, it appears that using full AO compensation in the absence of aero-optic effects improves the mean PIF by roughly 3-6 dB over no AO compensation at all ranges tested (Table 3). In the presence of aero-optic effects, however, the full AO compensation improves the mean PIF by 5-9 dB over that without AO compensation under the same turbulence conditions (Table 4). This is an improvement of roughly 1-2 dB over just tip-tilt at both Tx and Rx.

Table 3 Estimated statistical quantities associated with the downlink ORCA data beam for moderate-to-strong atmospheric conditions. Aero-optic effects are neglected. The estimates below are appropriate for Flight #2 conditions on May 16 when the gimbal angle of the aircraft turret was close to zero. Results are based on HAP model with M = 3.3 and $C_n^2(h_0) = 1.89\times10^{-13}$ m$^{-2/3}$. The transmitted power is assumed to be 33.8 dBm.

Moderate-to-Strong Turbulence without Aero-Optic Effects
DOWNLINK ANALYSIS

Model	*Range*	r_{0Tx}	r_{0Rx}	*SR Ground*	*PIB*	*PIF*
HAP-4/3 No AO	50 km	21.6 cm	9.8 cm	0.82	1.67 dBm	-12.0 dBm
HAP-4/3 w Tx &Rx Tip-Tilt	50 km	----	----	----	----	-9.5 dBm
HAP-4/3 w Full AO	50 km	----	----	0.99	1.67 dBm	-8.5 dBm
HAP-4/3 No AO	100 km	16.2 cm	7.9 cm	0.69	-7.7 dBm	-22.6 dBm
HAP-4/3 w Tx &Rx Tip-Tilt	100 km	----	----	----	----	-19.4 dBm
HAP-4/3 w Full AO	100 km	----	----	0.98	-7.7 dBm	-17.9 dBm
HAP-4/3 No AO	140 km	14.6 cm	7.2 cm	0.61	-13.2 dBm	-28.7 dBm
HAP-4/3 w Tx & Rx Tip-Tilt	140 km	----	----	----	----	-25.1 dBm
HAP-4/3 w Full AO	140 km	----	----	0.98	-13.2 dBm	-23.5 dBm
HAP-4/3 No AO	170 km	13.7 cm	6.8 cm	0.56	-16.8 dBm	-32.7 dBm
HAP-4/3 w Tx & Rx Tip-Tilt	170 km	----	----	----	----	-28.9 dBm
HAP-4/3 w Full AO	170 km	----	----	0.97	-16.8 dBm	-27.1 dBm

Table 4 Estimated statistical quantities associated with the downlink ORCA data beam for moderate-to-strong atmospheric conditions. Aero-optic effects are included. The estimates below are appropriate for Flight #2 conditions on May 16 when the gimbal angle of the aircraft turret was close to 90 deg. Results are based on HAP model with M = 3.3 and $C_n^2(h_0) = 1.89\times10^{-13}$ m$^{-2/3}$. The transmitted power is assumed to be 33.8 dBm.

Moderate-to-Strong Turbulence with Aero-Optic Effects
DOWNLINK ANALYSIS

Model	*Range*	r_{0Tx}	r_{0Rx}	*SR Ground*	*PIB*	*PIF*
HAP-4/3 No AO	50 km	21.6 cm	9.8 cm	0.48	-0.6. dBm	-14.3 dBm
HAP-4/3 w Tx Tip-Tilt	50 km	----	----	0.75	1.3 dBm	-12.4 dBm
HAP-4/3 w Tx & Rx Tip-Tilt	50 km	----	----	----	----	-9.9 dBm
HAP-4/3 w Full AO	50 km	----	----	0.99	1.3 dBm	-8.8 dBm
HAP-4/3 No AO	100 km	16.2 cm	7.9 cm	0.32	-11.1 dBm	-26.0 dBm
HAP-4/3 w Tx Tip-Tilt	100 km	----	----	0.60	-8.3 dBm	-23.2 dBm
HAP-4/3 w Tx & Rx Tip-Tilt	100 km	----	----	----	----	-19.9 dBm
HAP-4/3 w Full AO	100 km	----	----	0.98	-8.3 dBm	-18.4 dBm
HAP-4/3 No AO	140 km	14.6 cm	7.2 cm	0.25	-17.1 dBm	-32.6 dBm
HAP-4/3 w Tx Tip-Tilt	140 km	----	----	0.52	-13.9 dBm	-29.4 dBm
HAP-4/3 w Tx & Rx Tip-Tilt	140 km	----	----	----	----	-25.7 dBm
HAP-4/3 w Full AO	140 km	----	----	0.98	-13.9 dBm	-24.0 dBm
HAP-4/3 No AO	170 km	13.7 cm	6.8 cm	0.21	-21.0 dBm	-36.9 dBm
HAP-4/3 w Tx Tip-Tilt	170 km	----	----	0.47	-17.6 dBm	-33.5 dBm
HAP-4/3 w Tx & Rx Tip-Tilt	170 km	----	----	----	----	-29.7 dBm
HAP-4/3 w Full AO	170 km	----	----	0.97	-17.6 dBm	-27.7 dBm

3.2 Mean PIF and Fade Statistics for ORCA Data Beam: Data Analysis

Mean PIF Analysis: Ref. [2]

PIF data recorded during Flight #1 on May 17 and reported in Ref. [2] showed a mean PIF reading of roughly -18 dBm to -20 dBm when the aircraft was traveling head-on toward the receiver (zero gimbal angle) at a range of approximately 100 km (see Fig. 10 in Ref. [2]). When the aircraft was traveling nearly transverse (side-on) to the propagation path, the data in Figs. 10 and 17 of Ref. [2] show roughly a 4 dB loss in mean PIF (i.e., -22 dBm to -24 dBm). This PIF data for side-on as compared with head-on is similar to the moderate-to-strong turbulence conditions provided in the first row of Tables 3 and 4 at the 100 km range. That is, Table 3 lists head-on mean PIF as -22.6 dBm with no AO compensation and Table 4 lists side-on mean PIF as -26.0 dBm, a decrease of 3.4 dB caused by aero-optic effects. However, with full AO compensation the mean PIF in Tables 3 and 4 are -17.9 dBm and -18.4 dBm, respectively.

At ranges of 140 km and 170 km during Flight #1 on May 17, the mean PIF reported in Ref. [2] was generally around -27.7 dBm and -30.5 dBm, respectively (see Figs. 10 and 17 in Ref. [2]). These mean PIF values are close to the theoretical values shown in the third row of Table 4 at each range (viz., -25.7 dBm and -29.7 dBm, respectively), based on tip-tilt compensation at both ends of the link. However, there is insufficient data to draw a definite conclusion about the effectiveness of the full AO compensation system during testing.

Mean PIF Analysis and Fading Analysis for Flight #1 on May 17, 2009: UCF

The UCF team received data from NGC and performed further analysis on the NTTR data in order to determine mean PIF values and fade statistics over a wider sample of the data than presented in Ref. [2]. Shown below in Figs. 9-11 are calculations of the mean PIF (Fig. 9), mean fade time below -41 dBm (Fig. 10), and mean packet loss per fade as a function of range (Fig. 11).

To calculate mean fade time the team located points where the data dropped below -41 dBm and then recorded the elapsed time until it rose above -41 dBm. For each data segment all of these times were computed and then averaged, producing the numbers referred to as mean fade times. The values for mean packet loss assume a nominal data rate of 5 Gbps and a packet length of 8000 bits. After mean fade time is computed, it is multiplied by the data rate and divided by the packet length producing a number that represents the number of packets lost in a fade of average length. For mean fade time and packet loss computations any data segment whose mean PIF was below -50 dBm was discarded as the data is dominated by "system level" failures that are not believed to be caused by atmospheric effects. Data analysis was done by breaking the data into small segments; segment lengths of 5 seconds, 10 seconds, and 20 seconds were used; however, only a small selection of the analysis is displayed for conciseness.

Atmospheric conditions were based on measurements made on May 16, not May 17. The assumed laser power at the transmitter is 33.8 dBm in (*a*) and 35.8 dBm in (*b*). The solid blue curve is based on aero-optic effects with the AO compensation system turned off. The blue dashed-dotted curve corresponds to no aero-optic effect and no AO compensation, and the red dotted curve corresponds to the full AO compensation system turned on with or without aero-optic effects. Based on these theoretical results, it appears that full AO compensation can improve the mean PIF by 5-9 dB (depending on range) over no AO compensation when aero-optic effects are present.

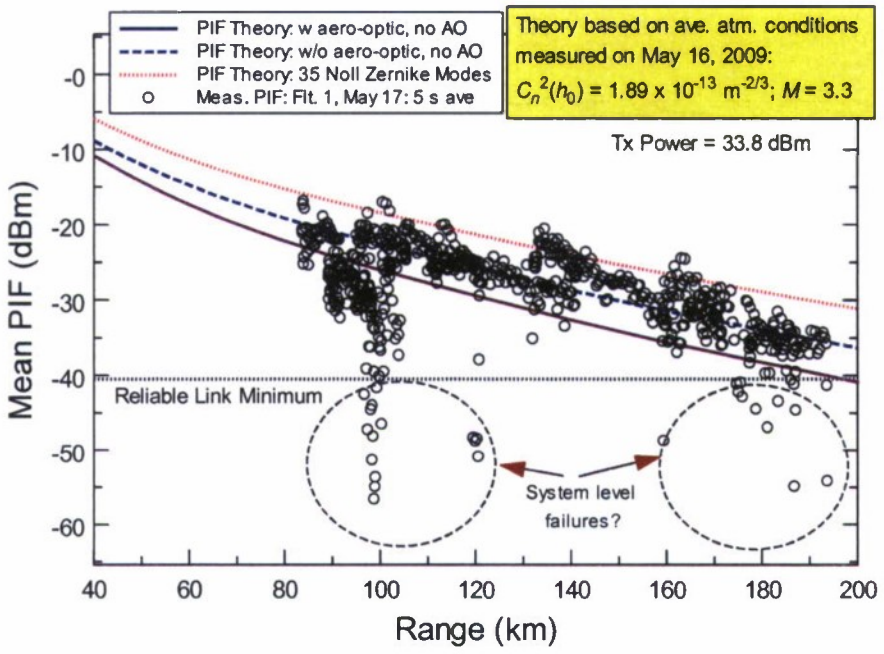

(*a*)

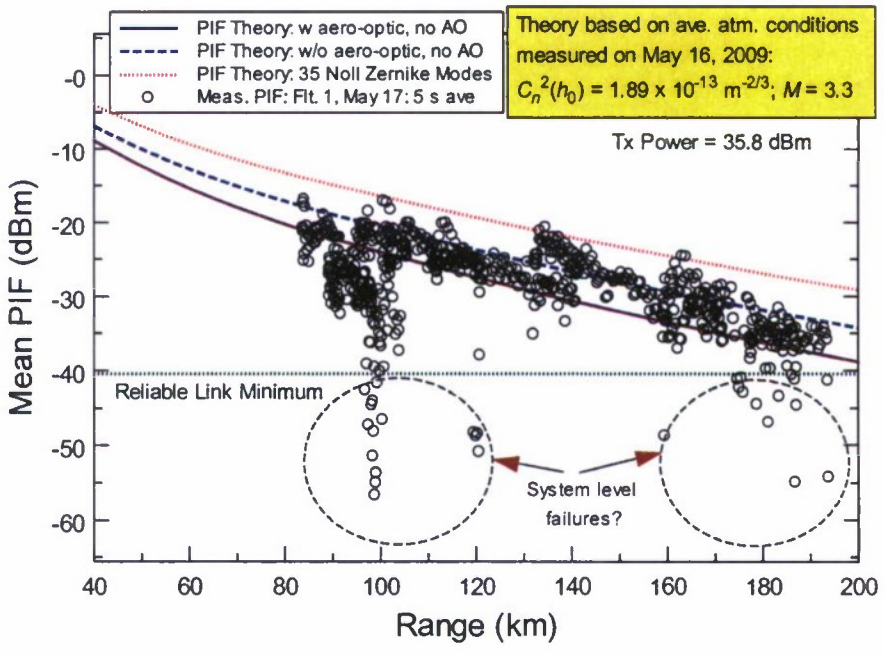

(*b*)

Figure 9 Mean PIF data taken during Flight #1 on May 17, 2009. The data represents measurements made over (*a*) a 5 s timeframe with 33.8 dBm of Tx power and (*b*) a 5 s timeframe with 35.8 dBm of Tx power. The lower theoretical curves are shown with and without the aero-optics effect and AO compensation off. The red dotted curve corresponds to full AO compensation with or without aero-optic effects.

The mean fade time shown in Fig. 10 lies mostly below 2 ms and much of it below 1 ms. The mean packet loss per fade is shown in Fig. 11 (5 s average only). The mean packet loss per fade is based on a data rate of 5 Gbps.

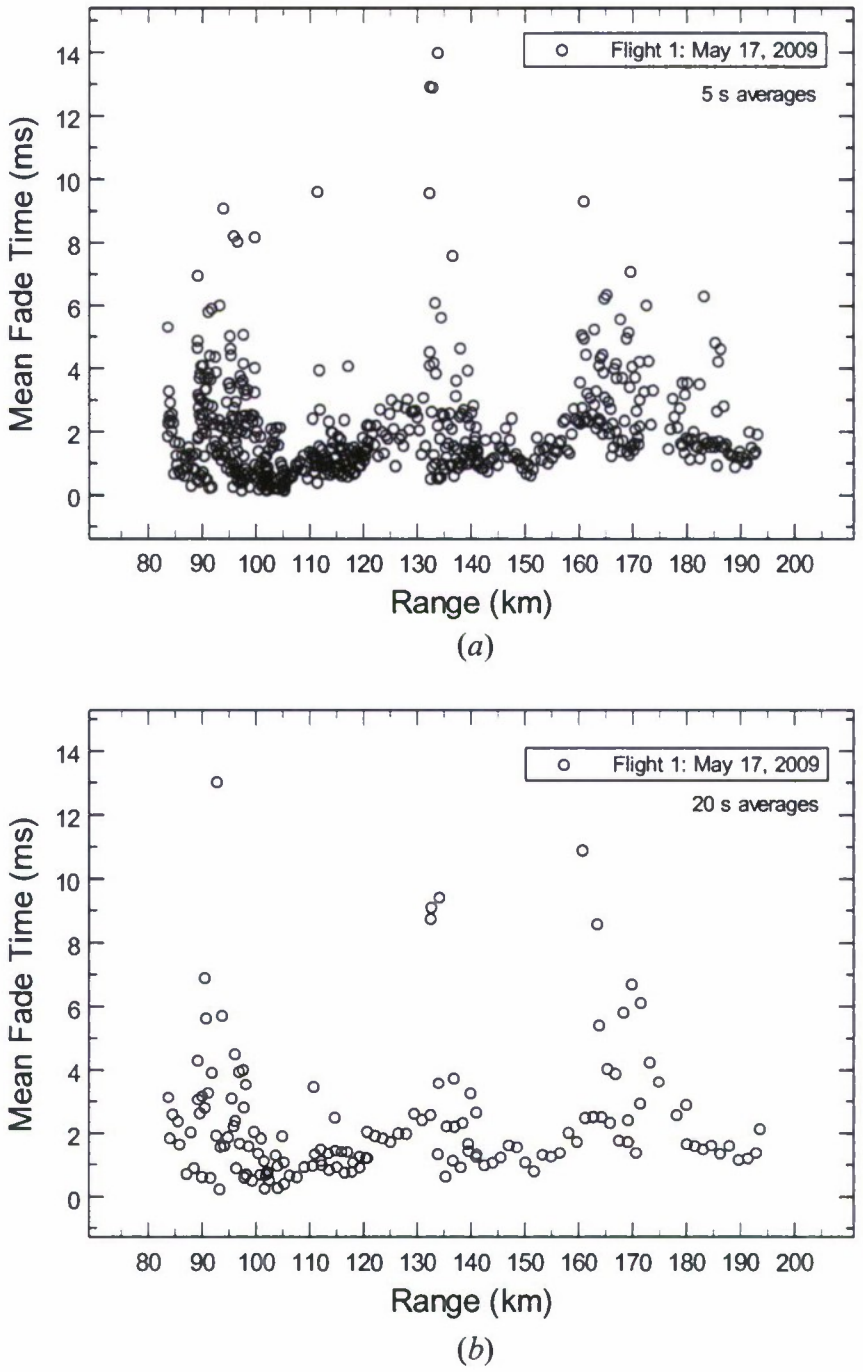

Figure 10 Mean fade time below -41 dBm in ms calculated from PIF data taken during Flight #1 on May 17, 2009. The data represents mean fade measurements made over (*a*) a 5 s timeframe and (*b*) a 20 s timeframe.

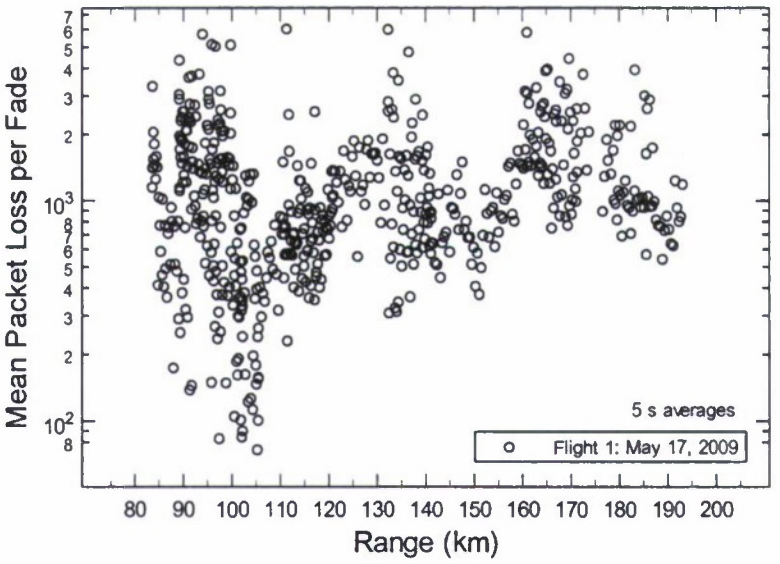

Figure 11 Mean packet loss per fade calculated from PIF data taken during Flight #1 on May 17, 2009. The data represents a data rate of 5 Gbps made over a 5 s timeframe.

To better understand the orientation of the aircraft during the measurement period, we show in Fig. 12 the mean gimbal angle as a function of range for Flight #1 on May 17. The beginning minutes of the flight between 105 km and 90 km led to values of the mean PIF below -25 dBM shown by the yellow circles in Fig. 12. Later on during the flight, the lavender circles indicate the gimbal angle when the mean PIF fell below -41dBm.

The mean PIF as a function of gimbal angle is shown in Fig. 13. In (*a*), the range is between 84 km and 105 km during the first part of the flight. In (*b*), the range is between 120 km to 171 km. In general, one can see a somewhat higher mean PIF near gimbal angle zero as compared with gimbal angle near 90 degrees.

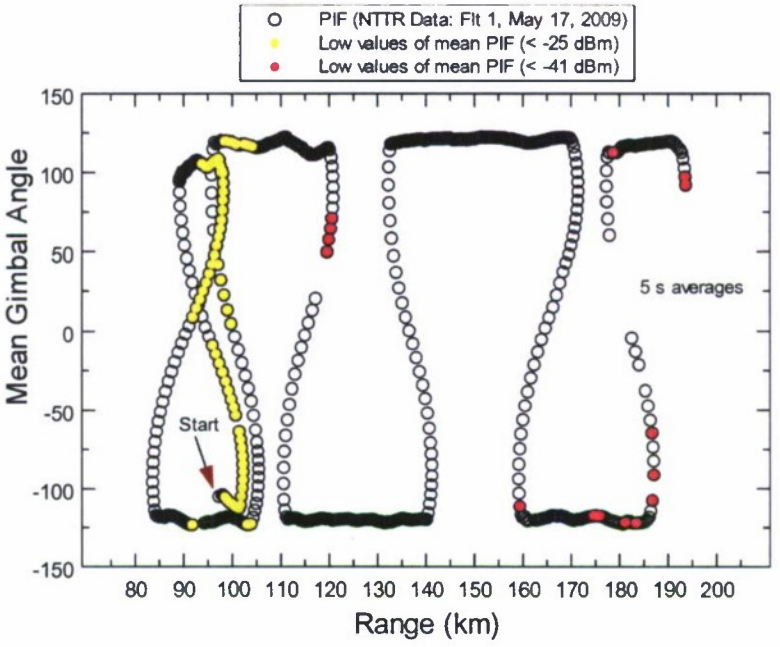

Figure 12 Plot of the mean gimbal angle as a function of range for Flight #1 on May 17, 2009 at NTTR.

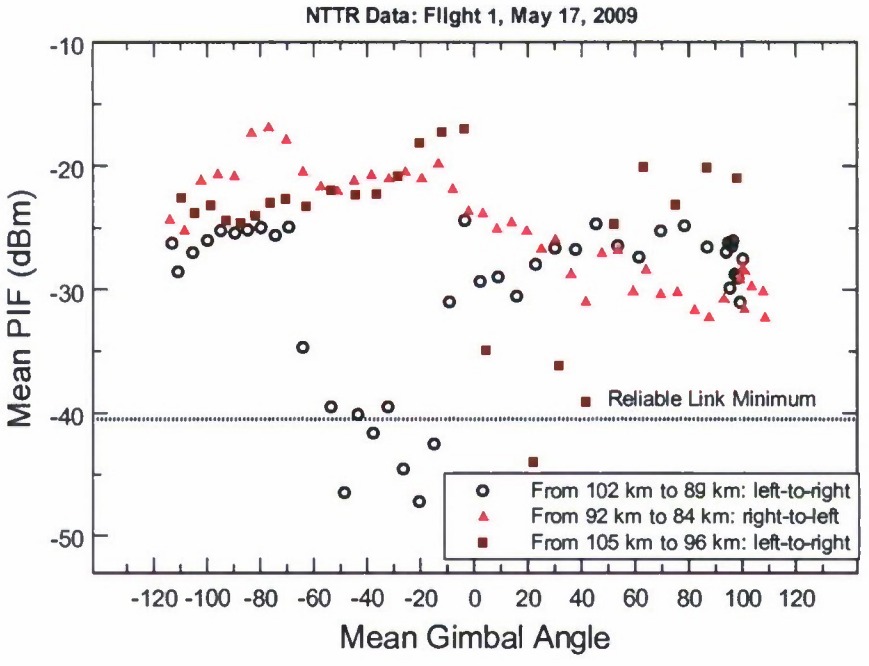

(*a*)

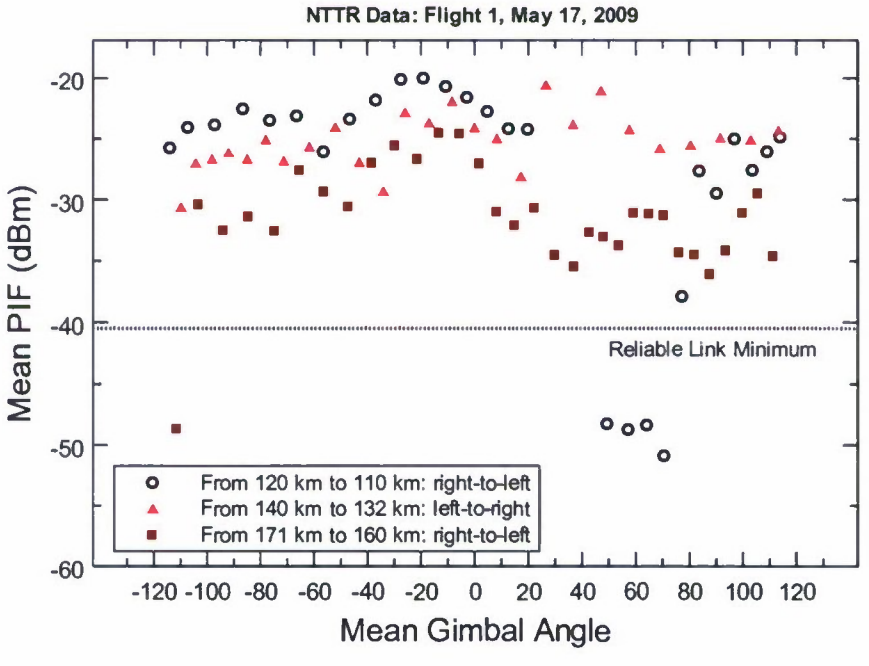

(*b*)

Figure 13 Plot of the mean PIF as a function of gimbal angle for Flight #1 on May 17, 2009 at NTTR. In (*a*), the range is between 84 km and 105 km and in (*b*), the range is between 120 km and 171 km.

4. PAX RIVER ANALYSIS: UPLINK DATA BEAM

Before testing the ORCA system at NTTR, a preliminary test of the system was performed at PAX River from 2:00-4:00 AM on May 12, 2009. During the PAX River testing, no atmospheric conditions were measured along the propagation path nor were any ground level C_n^2 measurements performed. However, NGC determined from the WRF model that the Fried parameter r_0 for an uplink beam from ground to the aircraft at 70-km range was around 23 cm. To obtain this result from the HAP model (1), we use the -2/3 power law, assume the ground-level $C_n^2(h_0) = 1\times10^{-15}$ m$^{-2/3}$ and background turbulence described by $M = 0.75$. Nonetheless, macro atmospheric parameters on that day suggest that $M = 0.5$ and $C_n^2(h_0) = 0.83\times10^{-15}$ m$^{-2/3}$. We also made the assumption that $h_s \sim 0$ and $h_0 = 1$m in the HAP model. The altitude of the aircraft above sea level was generally between 9-10 kft. Based on these later conditions, the Fried parameter at the aircraft is r_0 = 29 cm at 70-km range. The assumed beam power transmitted is 31.2 dBm for the theoretical analysis given in Table 5 below.

4.1 Irradiance Variance and Scintillation Index vs Gimbal Angle

It was not known initially whether the PAX River data obtained from NGC was for an uplink or downlink propagation path. After some initial discussion with NGC and UCF analysis of the data, UCF obtained the conclusion that the PAX River data taken on May 12, 2009 was for an uplink propagation path during nighttime hours (2-4 AM). From the data we show the irradiance variance and scintillation index plotted as a function of gimbal angle in Figs. 14-16. Theoretically, we wouldn't expect to see any aero-optics effects for an uplink beam from ground to aircraft. The data for the irradiance variance shown in Figs. 14-16 seem to substantiate that conjecture, unlike the variance data shown in Fig. 3 above for the downlink beacon beam measured at NTTR. In Fig. 14 we show the variance and scintillation index for ranges over 32-42 km. Similar graphs are shown in Figs. 15 and 16 for ranges of 35-55 km and 70-72.5 km, respectively.

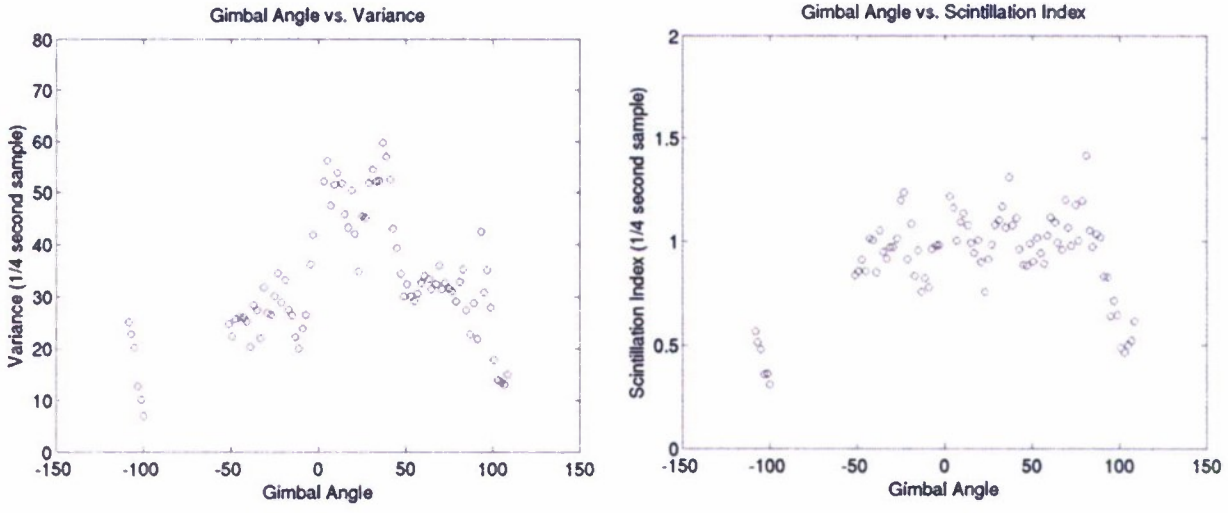

Figure 14 Irradiance variance and scintillation index plotted as a function of gimbal angle for uplink data at PAX River at ranges of 32-42 km.

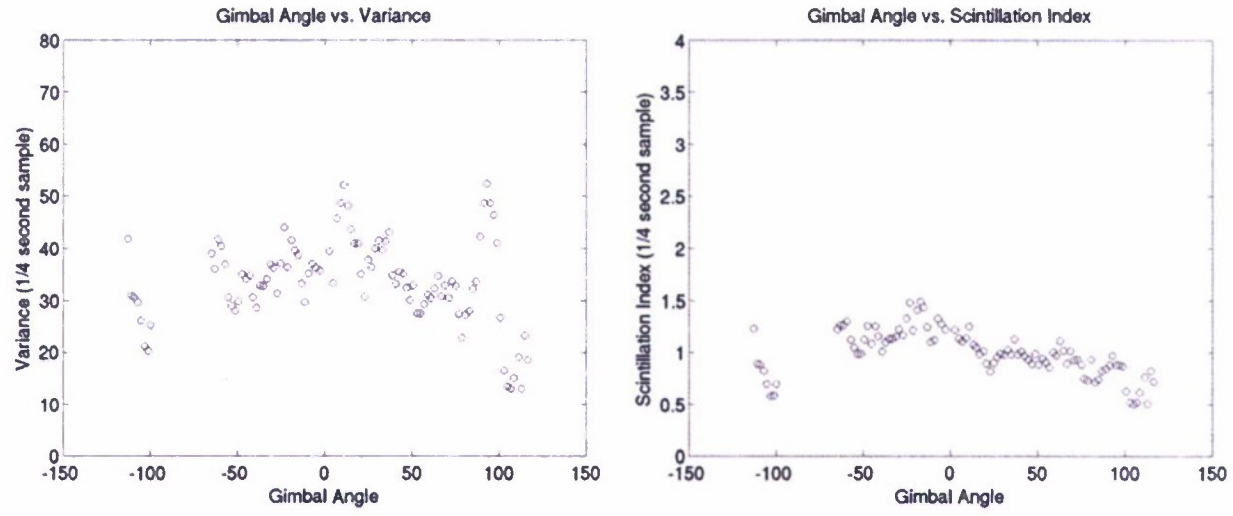

Figure 15 Irradiance variance and scintillation index plotted as a function of gimbal angle for uplink data at PAX River at ranges of 35-55 km.

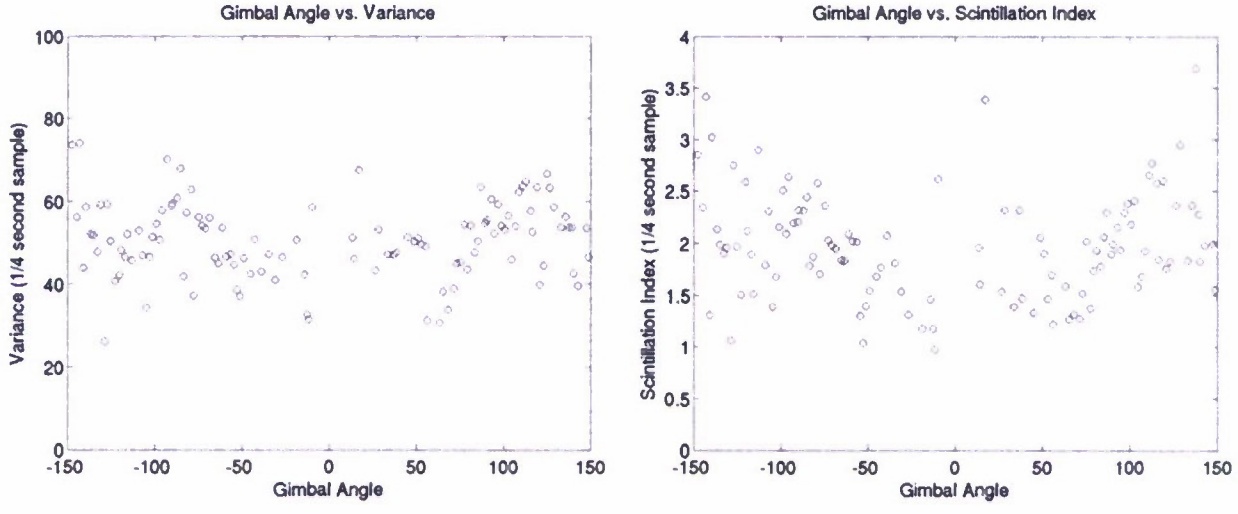

Figure 16 Irradiance variance and scintillation index plotted as a function of gimbal angle for uplink data at PAX River at ranges of 70-72.5 km.

4.2 AO Compensation for ORCA Data Beam

In Table 5 below we again list the same parameters as those in Tables 3-4, but this time for the uplink beam at PAX River with aircraft altitude assumed to be 9,500 ft. We assume the transmittance parameter for the atmosphere is $\tau_{\text{atm}} = e^{-0.007L}$, where range L is in km, the optics transmittance is $\tau_{\text{opt}} = 0.6$, and that $f_{\text{Airy}} = 0.2$. We also used the parameter $4/\beta^2$ to take into account the possible spot size mismatch at the fiber entrance. The spot size mismatch at the optical fiber amounts to an additional 1-2 dB loss in mean PIF without full AO. Again, aero-optic effects are negligible for the uplink beam.

Table 5 PAX River theoretical modeling from ground-to-air link over various ranges. Aero-optic effects are negligible. Results are based on $h_0 = 1$ and $M = 0.5$ in HAP model with ground level refractive-index fluctuations $C_n^2(h_0) = 0.83 \times 10^{-15}$ m$^{-2/3}$. The nighttime model is based on -2/3 power law near the ground. The transmitted power is assumed to be 31.2 dBm.

Moderate Turbulence without Aero-Optic Effects
UPLINK ANALYSIS

Model	Range	r_{0Tx}	r_{0Rx}	SR Aircraft	PIB	PIF
HAP-4/3 No AO	35 km	26 cm	44 cm	0.83	4.3 dBm	-5.8 dBm
HAP-4/3 w Tx & Rx Tip-Tilt	35 km	----	----	0.94	4.8 dBm	-4.7 dBm
HAP-4/3 w Full AO	35 km	----	----	0.99	4.8 dBm	- 4.4 dBm
HAP-4/3 No AO	50 km	21 cm	36 cm	0.77	0.4 dBm	-10.0 dBm
HAP-4/3 w Tx & Rx Tip-Tilt	50 km	----	----	0.91	1.2 dBm	-8.4 dBm
HAP-4/3 w Full AO	50 km	----	----	0.99	1.2 dBm	- 8.1 dBm
HAP-4/3 No AO	70 km	17 cm	29 cm	0.70	-3.5 dBm	-14.3 dBm
HAP-4/3 w Tx & Rx Tip-Tilt	70 km	----	----	0.88	-2.5 dBm	-12.3 dBm
HAP-4/3 w Full AO	70 km	----	----	0.99	-2.5 dBm	- 11.7 dBm

From the table it can be seen that tip-tilt corrections at Tx and Rx increase the mean PIF by 1-2 dB over no AO, and full AO compensation increases the mean PIF by 2-3 dB over no AO. Thus, full AO increases the mean PIF by approximately 1-2 dB over tip-tilt alone on the uplink path.

4.3 Mean PIF and Fade Statistics for ORCA Data Beam: Data Analysis

PIF data collected at PAX River on the uplink beam from ground to aircraft has been analyzed by the UCF team. In Figs. 17-19 we plot the mean PIF vs range, mean gimbal angle vs range, mean fade time, and mean packet loss per fade for 5 s samples of the PAX River data. Along with the data in Fig. 17 is a theoretical curve based on tip-tilt corrections as found in Row 2 of Table 5. In addition, the blue dashed-dotted curve corresponds to the AO compensation system turned off and the red dotted curve corresponds to the full AO compensation system turned on. The ground conditions do not influence Fried's parameter very much on an uplink path, only the turbulence close to the receiver on the aircraft. Much of the mean PIF data in Fig. 17 for ranges less than 55 km are 2-3 dB higher than the solid theoretical curve, and also higher than the full AO compensation curve. Atmospheric conditions were assumed to be the same at 35-55 km ranges as for the 70-km range, but, based on the data, this may not be true. Nonetheless, the data seem to support the fact that the full AO compensation system was fully operational during the PAX River testing.

In Fig. 18 we plot the mean gimbal angle vs range. Because the data in Fig. 17 seems to break into two distinct groups (one higher than the other), we colored the mean gimbal angle data in Fig. 18 to show orientation of the aircraft during the lower readings.

The mean fade times shown in Fig. 19(a) are much lower in general than corresponding fade times found at NTTR. Of course, the ranges at PAX were generally shorter and we believe the background turbulence was also considerably weaker than that at NTTR (i.e, $M = 0.5$ at PAX whereas $M = 3.3$ at NTTR). Hence, we note that in general the mean PIF was much higher than that at NTTR whereas the mean fade time and packet losses were much lower than that at NTTR.

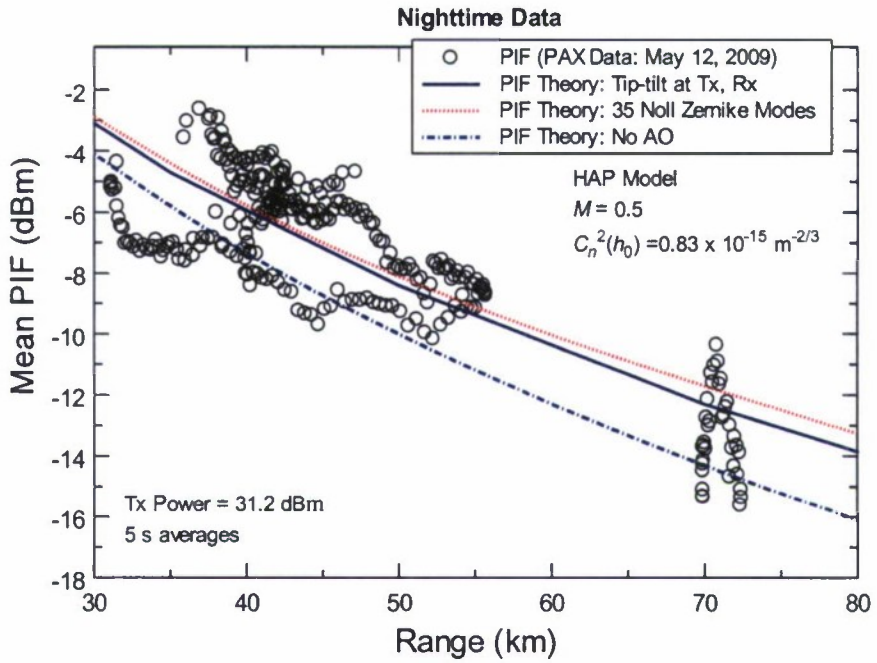

Figure 17 Mean PIF data taken during preliminary flights on May 12, 2009, at PAX River. The data represents measurements made over a 5 s timeframe. The Tx power is 31.2 dBm.

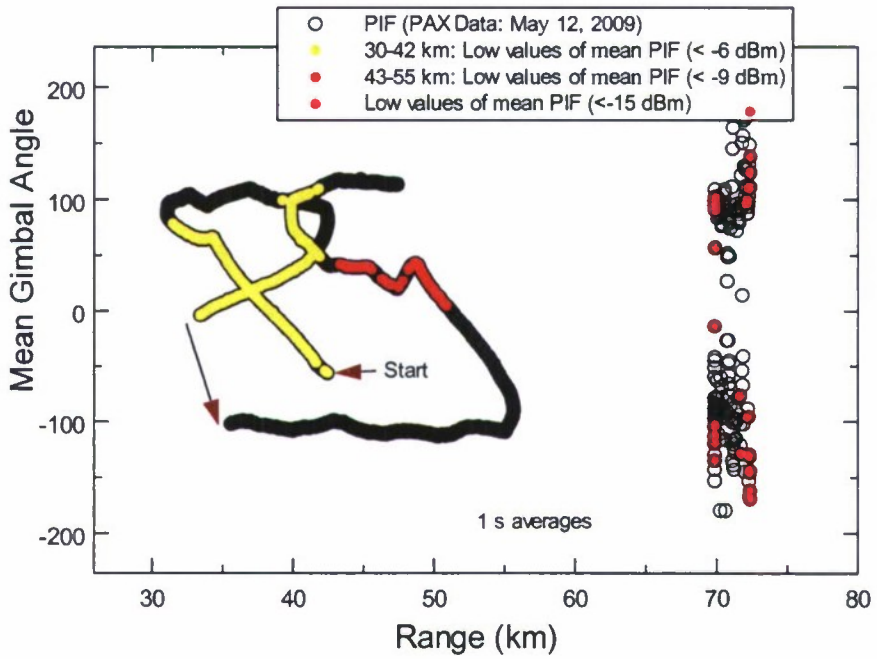

Figure 18 Mean gimbal angle data taken during preliminary flights on May 12, 2009, at PAX River. The data represents measurements made over a 5 s timeframe. The Tx power is 31.2 dBm.

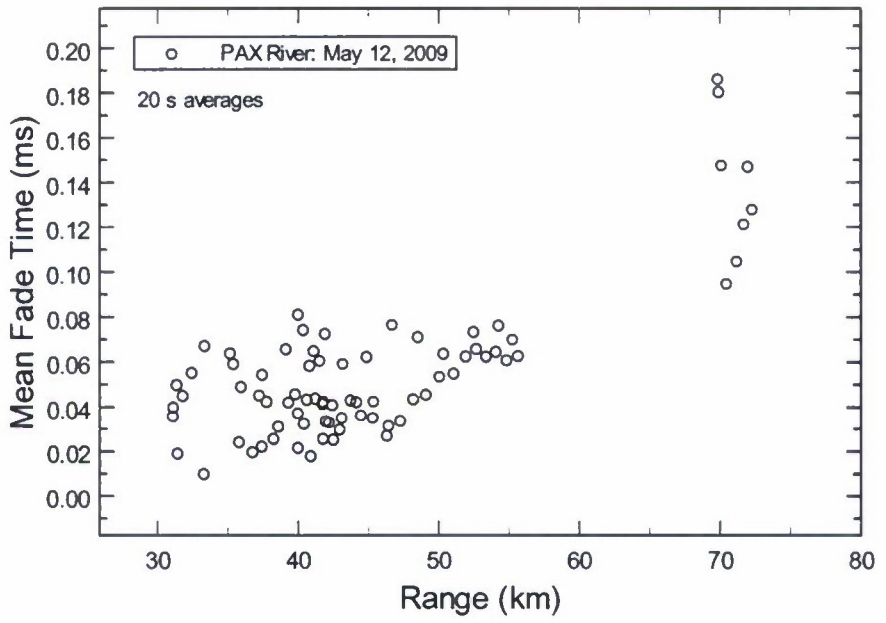

Figure 19(*a*) Mean fade time below -41 dBm in ms calculated from PIF data taken during PAX River testing on May 12, 2009. The data represents mean fade measurements made over a 20 s timeframe.

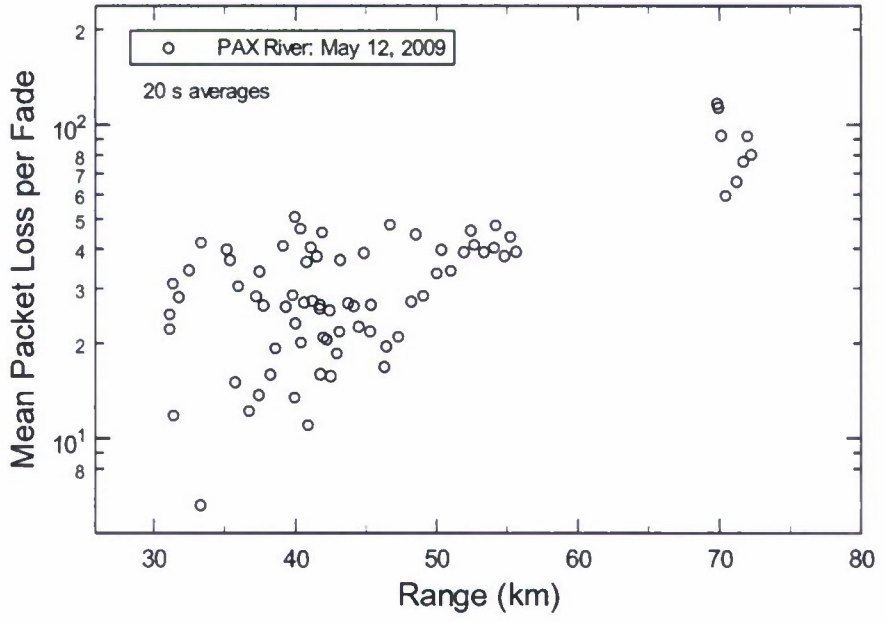

Figure 19(*b*) Mean packet loss per fade calculated from PIF data taken during PAX River testing on May 12, 2009. The data represents a data rate of 5 Gbps made over a 20 s timeframe.

5. AIR-TO-AIR THEORETICAL AO ANALYSIS

The NTTR and PAX River analysis suggests that a full AO compensation system often provides only a modest improvement in mean PIF over that of a tip-tilt compensation system for ranges exceeding 50 km. In this section we wish to further examine the comparison of a full AO system with a tip-tilt only system over an air-to-air link as a function of range.

In Fig. 20 we show theoretical plots of the mean PIF as a function of range for no AO compensation system, a tip-tilt compensation system, and a full AO compensation system. We assume the background turbulence in the HAP model (3) is characterized by $M = 25$, corresponding to very strong background turbulence. The ground level refractive-index structure parameter is taken as $C_n^2(h_0) = 1.7 \times 10^{-14}$ m$^{-2/3}$. Aero-optic effects have been neglected in this analysis. The transmitted power is assumed to be 1.0 Watt (30 dBm). The theory suggests there is only 1-3 dB improvement in the full AO compensation system over just tip-tilt for ranges 50-200 km. However, this is a 12 dB gain over no AO at 200 km range.

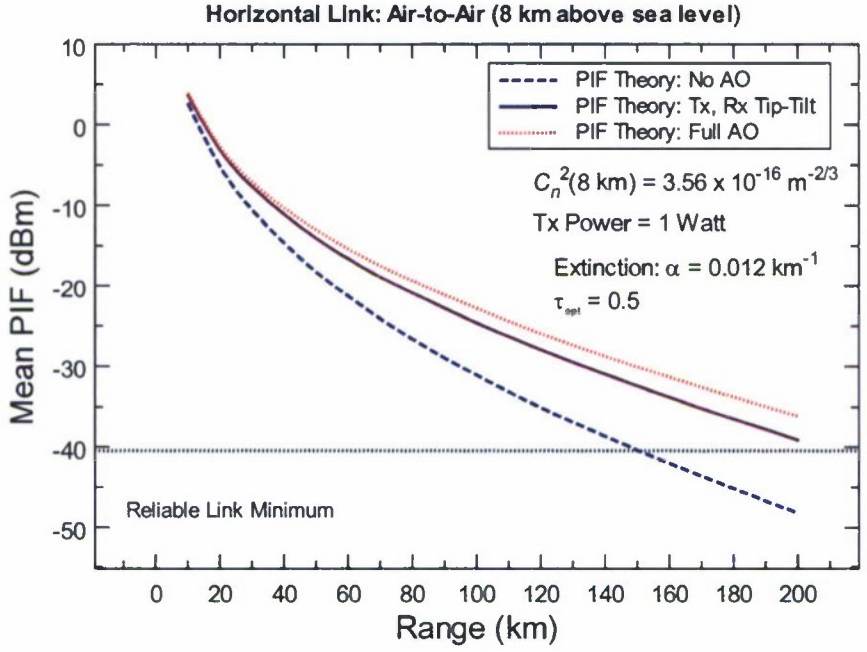

Figure 20 Theoretical prediction of mean PIF as a function of range for an air-to-air propagation path.

6. IRON-T2 TESTING IN HAWAII

Over the past 5 years, DARPA and the U.S. Air Force Research Laboratory (AFRL) have conducted field trials in an effort to validate optical links over long distances. Before PAX River and NTTR, testing was conducted on the Integrated RF/Optical Networked Tactical Targeting Networking Technologies (IRON-T2) system over a 147-km path between Haleakala and Mauna Loa in Hawaii. Data taken during the middle part of the day on October 16, 2008 has been analyzed by the UCF team. Mean PIF values as a function of local time of day are presented in Fig. 21 and mean fade time as a function of local time of day presented in Fig. 22. Ground level C_n^2 values on each mountain were not available so no theoretical curves are presented along with the measured PIF data. Mean fade times were all under 0.5 ms.

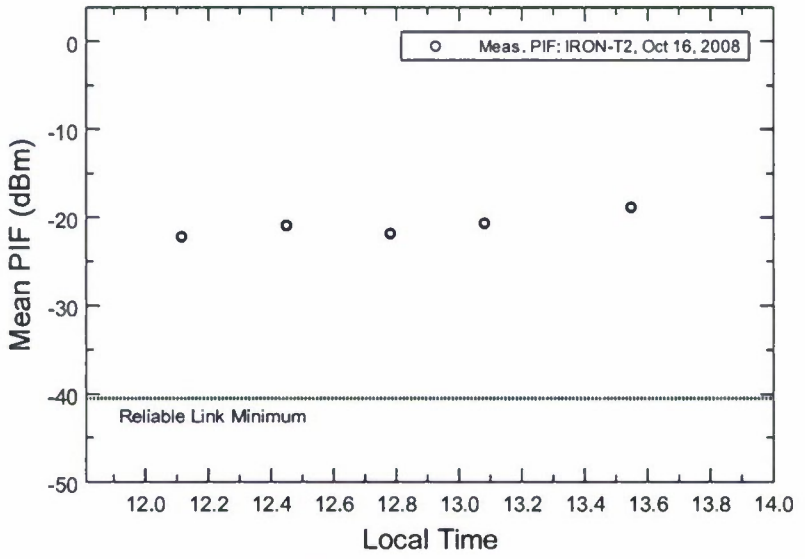

Figure 21 Measurements for IRON-T2 leading to mean PIF as a function of local time of day in Hawaii.

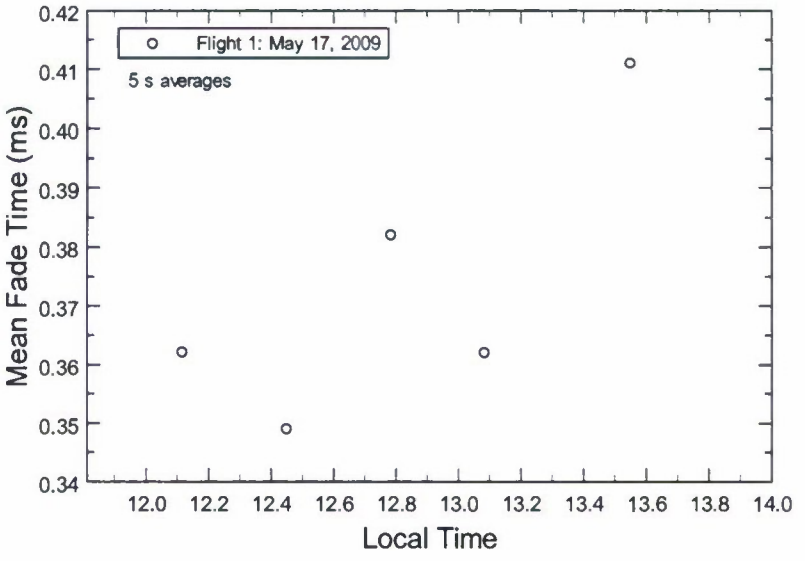

Figure 22 Measured mean fade time as a function of range for an air-to-air propagation path.

We also calculated the pdf and cdf of the IRON-T2 data. Shown below in Fig. 23 are two such plots, also depicting the mean and median values as well as the 99% fade depth of the PIF.

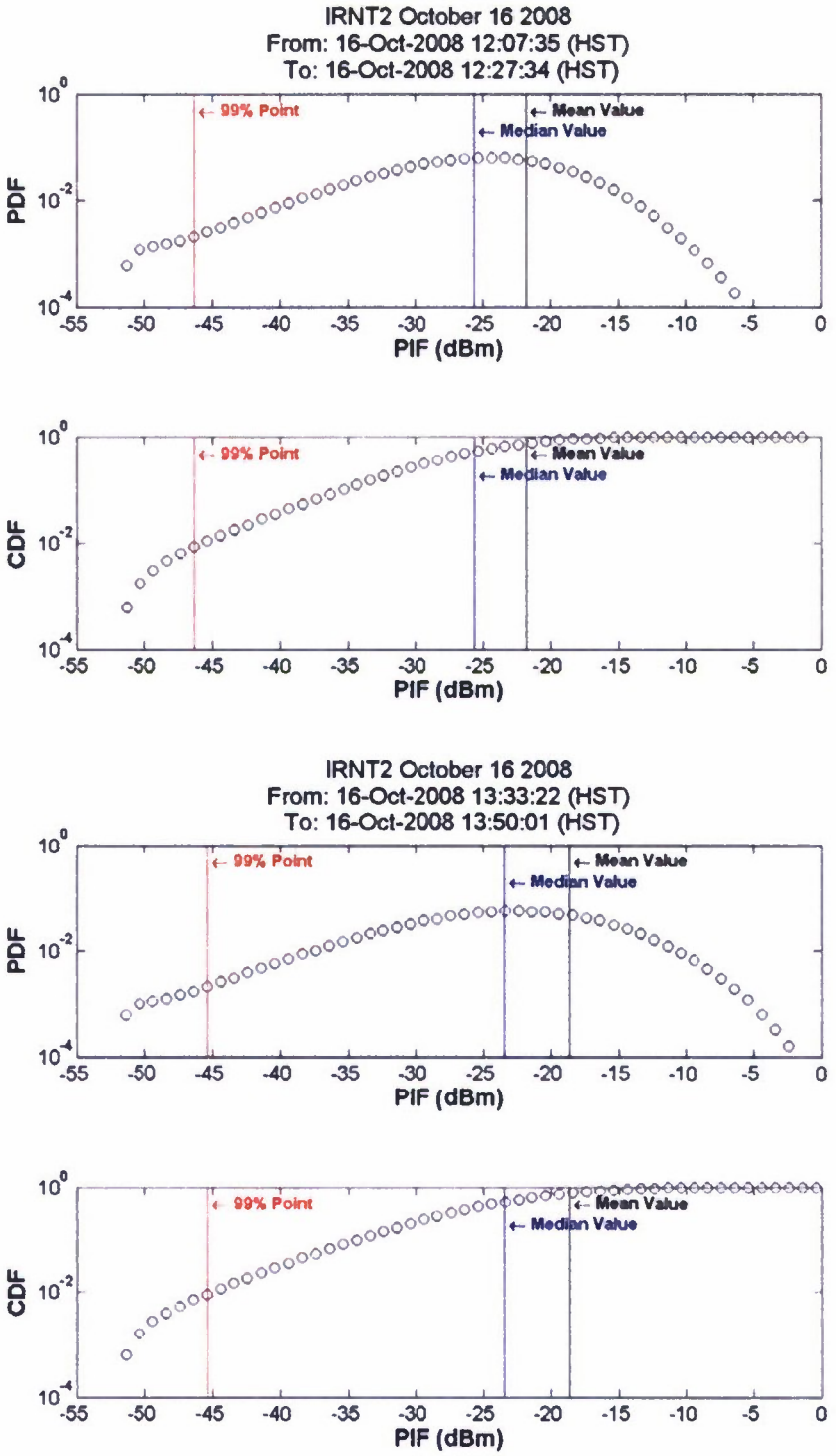

Figure 23 Measured pdf and cdf as a function of PIF for the 147-km IRON-T2 propagation path in Hawaii. Also shown are the mean PIF, the median PIF, and the 99% fade depth.

7. KOPEIKA PREDICTIVE MODELS COMPARED WITH ANTELOPE PEAK SCINTILLOMETER DATA

Over the years the general approach to understanding turbulence through the interaction between atmospheric optics and meteorology has been based on micrometeorology, using point measurements of local gradients, wind shear, and other parameters. However, to characterize atmospheric turbulence over long distances it is best to use macroscale parameters such as air temperature, wind speed and direction, and relative humidity, all of which do not vary too greatly with distance. Bendersky, Kopeika, and Blaunstein [6] have recently introduced a simple predictive meteorological C_n^2 model (the BKB model) that is a small variation of a similar model previously introduced by Kopeika [7]. In the analysis below we use macroscale atmospheric parameters measured at Antelope Peak on May 16, 2009 and compare the values of C_n^2 predicted by these models with scintillometer values actually measured at Antelope Peak during the same time period.

Macroscale meteorological data were collected over a period of two and a half days atop Antelope Peak, located within the Nevada Test and Training Range (NTTR). Figure 24 shows Antelope Peak with respect to the Tonopah Test Range Airport and other local mountain peaks. Scintillometers were set up near the summit of Antelope Peak over a path distance of 65 meters, at heights of 1 and 1.7 meters. The weather station was placed nearby, approximately 5 meters from the transmitting scintillometers. Although it is preferred to use a longer path length with these instruments, a longer distance was not possible due to space constraints on the mountain. The jagged terrain of the optical path between the scintillometer transmitter and receiver pairs consisted mostly of dirt, sand and rock. Mountains are known to exhibit somewhat reliable trends in the direction of prevailing wind, with tendency of rising up the windward side and falling down the leeward side. The purpose of this experiment is to test these predictive models under conditions which could be considered non-ideal to the original models. In progress, we are able to examine the hypothesis that optical conditions of a location can be approximated to a degree by local and/or remote meteorological measurements.

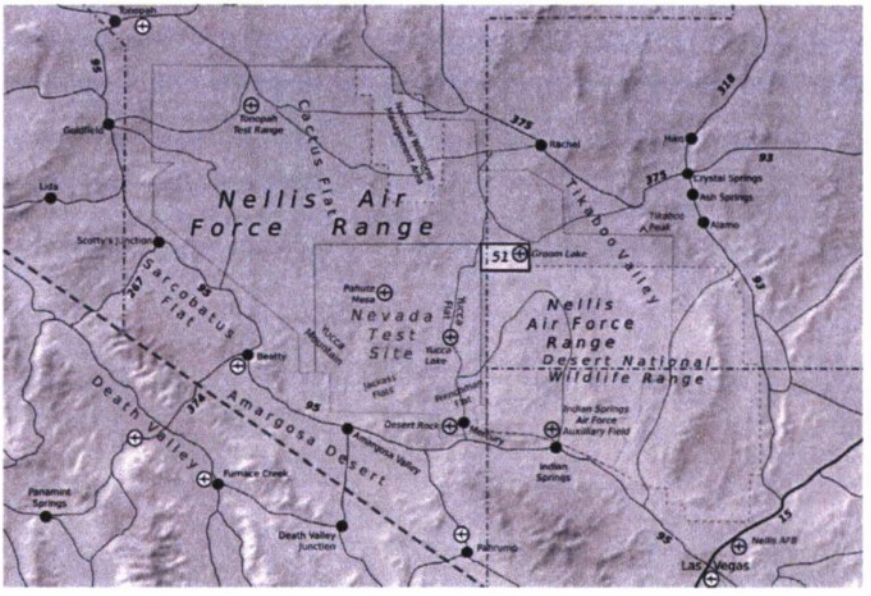

Figure 24 Location of Tonopah Test Range Airport with respect to general Nevada region and the Nellis Air Force Range.

7.1 Experimental Setup at Antelope Peak and Predictive C_n^2 Models

Figure 2 above (Section 2) shows the experimental setup for the scintillometer and weather instrumentation. The weather station consisted of three temperature sensors, a pyranometer for measurement of solar irradiance, and three "3-axis" anemometers to measure wind speed. In further detail, we utilized: an infrared sensor measuring ground-level temperature, a relative humidity and temperature sensor located at 1.5 meters, and another temperature sensor at 2.5 meters. Wind speed was measured by anemometers capable of resolving the wind speed vector into three orthogonal components at heights of 1, 2 and 2.6 meters. By taking a measure of the temperature and wind gradient, we are able to average the gradient to obtain more consistent temperature and wind values to input into the model. Temperature, relative humidity and solar irradiance probes were manufactured by Campbell Scientific and their data were recorded by a Campbell Scientific data logger. Computers, transmitters, and receivers were powered with blue-top marine batteries, while the instrumentation hooked up to the weather station (with exception of the 3-axis anemometers) was powered by Campbell Scientific data logger.

A few numerical models were utilized to predict the refractive-index structure parameter C_n^2 atop Antelope Peak. These models are based on the findings of Kopeika and his colleagues [6,7], deduced from several measurements made in southern Israel. The models are relatively simple and only require measurements of macro-meteorological parameters commonly taken by airports and weather stations. Several versions of the Kopeika model have been suggested in the past, and most of them have been considered for this comparison as we wish to determine which model most-properly describes the conditions that were observed.

Macroscopic weather model introduced by Bendersky, Kopeika, and Blaunstein (BKB model)

Only requires measurement of:

- Temperature (T), Kelvin
- Relative Humidity (RH), %
- Wind Speed (U), m/sec.
- Solar Flux (SF), kW/m^2
- Ground Albedo (A), unitless

Plus knowledge of the time of day relative to sunrise and sunset to compute the Temporal Weight Function (W, unitless) from table lookup.

Benefits:

- Opportunity to obtain data for experiments it was previously not measured
- Easily deployable weather instrumentation allows for accurate prediction of C_n^2 without expensive optical equipment

7.2 Kopeika Models

Several models have been introduced by Kopeika and his colleagues. Listed below are the models we examined. Also, the scaling model with altitude we use is that introduced by Walters and Kunkel [8].

Kopeika model

$$C_n^2 = 5.9 \times 10^{-14}\, W + f(T) + f(U) + f(RH) + f(SF) + f(TCSA) - 3.9 \times 10^{-13}$$

$$f(T) = 1.6 \times 10^{-15}\, T$$

$$f(U) = -3.7 \times 10^{-15} U + 1.3 \times 10^{-15}\, U^2 - 8.2 \times 10^{-17} U^3$$

$$f(RH) = -3.7 \times 10^{-15} RH + 6.7 \times 10^{-17} RH^2 - 3.9 \times 10^{-19} RH^3$$

$$TCSA = 9.69 \times 10^{-4} RH - 2.75 \times 10^{-5} RH^2 + 4.86 \times 10^{-7} RH^3 - 4.48 \times 10^{-9} RH^4 + 1.66 \times 10^{-11} RH^5 - 6.26 \times 10^{-3} \ln(RH) - 1.34 \times 10^{-6} SF^4 + 7.30 \times 10^{-3}$$

$$f(TCSA) = -1.8 \times 10^{-14} TCSA + 1.4 \times 10^{-14} TCSA^2$$

Alternative BKB model

$$C_n^2 = 3.8 \times 10^{-14}\, W + f(T) + f(U) + f(RH) - 5.3 \times 10^{-13}$$

$$f(T) = 2 \times 10^{-15}\, T$$

$$f(U) = -2.5 \times 10^{-15} U + 1.2 \times 10^{-15} U^2 - 8.5 \times 10^{-17} U^3$$

$$f(RH) = -2.8 \times 10^{-15} RH + 2.9 \times 10^{-17} RH^2 - 1.1 \times 10^{-19} RH^3$$

BKB model

$$C_n^2 = 3.8 \times 10^{-14}\, W + \frac{A \times 10^{-4}}{\exp(T)} + f(U) + f(RH) - 4.45 \times 10^{-14}$$

$$f(U) = 8 \times 10^{-16} U - 4 \times 10^{-18}\, U^2$$

$$f(RH) = -8 \times 10^{-16} RH + 5 \times 10^{-18} RH^2$$

Listed models predict C_n^2 for a height of 15-m above ground

Walters and Kunkel Height Scaling

$$\frac{C_n^2(h)}{C_n^2(h_0)} = \begin{cases} \left(\frac{h}{h_0}\right)^{-\frac{4}{3}}, & h_0, h \le .5h_i \\ \left(\frac{0.5h_i}{h_0}\right), & .5h_i \le h \le .7\,h_i \\ 2.9\left(\frac{.5h_i}{h_0}\right)^{\frac{4}{3}}\left(\frac{h}{h_i}\right)^{3}, & 0.7\,h_i \le h \le h_i \end{cases}$$

Where h_i is the height of the inversion layer above ground, h_0 is the height of the known C_n^2 and h is the height

-4/3 Height Scaling Power Law

$$C_n^2(h_1) = C_n^2(h_0)\left(\frac{h_0}{h_1}\right)^{4/3}$$

-2/3 Height Scaling Power Law

$$C_n^2(h_1) = C_n^2(h_0)\left(\frac{h_0}{h_1}\right)^{2/3}$$

h_0=15-m

h_1=1-m and 1.7-m

7.3 Scintillometer Data Compared with Predictive Models

In processing of the data, half-hour averages are utilized to smooth out the data. An average of this period is generally considered to yield the most reliable results in terms of macro-meteorological parameters such as relative humidity, temperature, wind speed and solar flux. The values of these parameters are expected to remain somewhat stable over short periods of time, but are expected to exhibit changes over longer periods (an hour or more). Additionally, there is need to consider a period of measurement that properly characterizes the conditions of a mountain peak. Since periodic wind gusts are known to occur atop mountains due to the aforementioned reasons and we wish to have a proper estimation of the average wind speed, we state a half-hour as a suitable period of time over which to average these measurements. Accordingly, these models produce a prediction for the refractive-index structure constant every half-hour. Since the devices used to directly measure the refractive-index structure constant produce a reading once every minute, it is necessary to average these measurements over a half-hour period as well to ensure the model and the measurement are on equal footing. With this stated, the results of the various models are shown below in Figs. 25-28 in comparison to measurements made by the Scintec SLS-20 scintillometers at heights of 1 meter and 1.7 meters. Figures 25 and 26 are daytime measurements using the HAP model with a -4/3 scaling law; Figures 27 and 28 are nighttime measurements using a -4/3 scaling law and a -2/3 scaling law, respectively, with the HAP model. Clearly, the -2/3 scaling law works best for nighttime measurements.

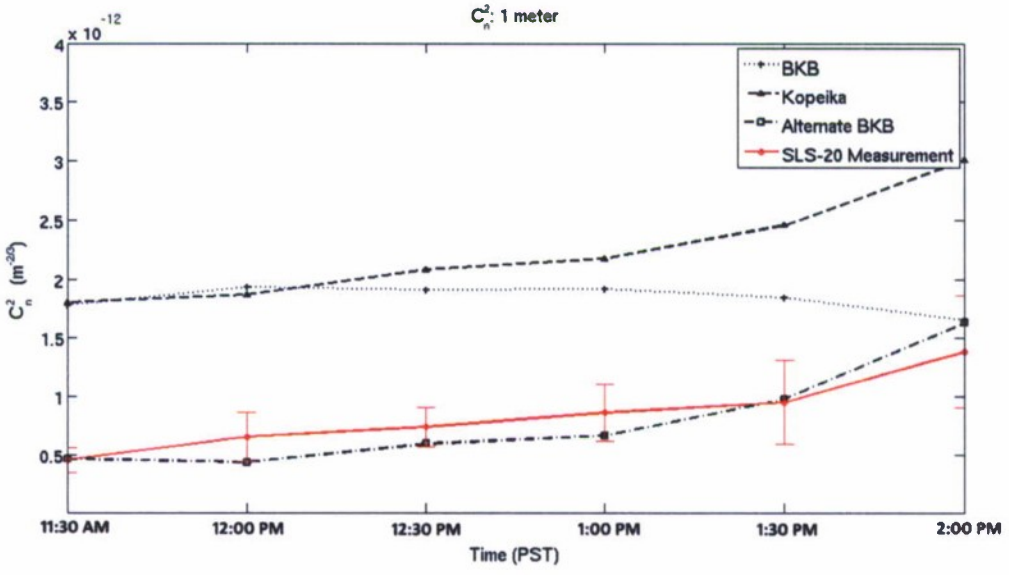

Figure 25 Comparison of C_n^2 Models 1 meter above ground (daytime).

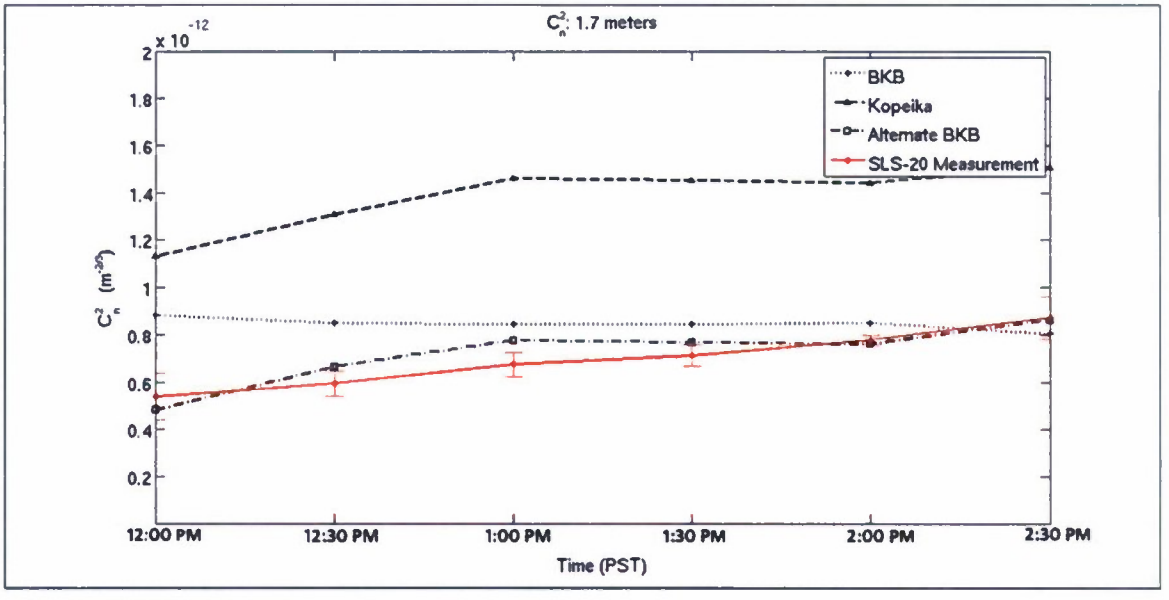

Figure 26 Comparison of C_n^2 Models 1.7 meters above ground (daytime).

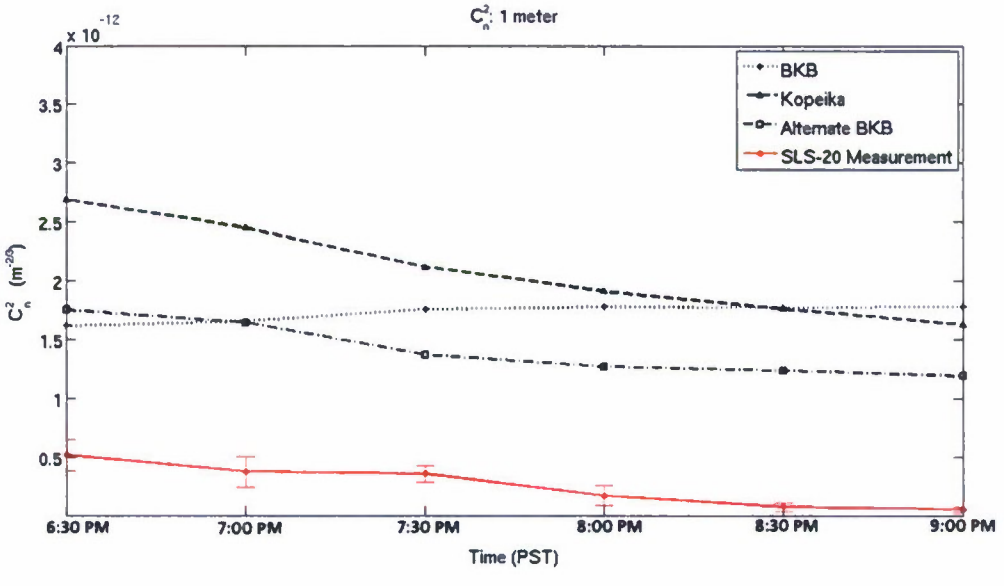

Figure 27 Comparison of C_n^2 Models 1 meter above ground (nighttime). Based on -4/3 HAP model.

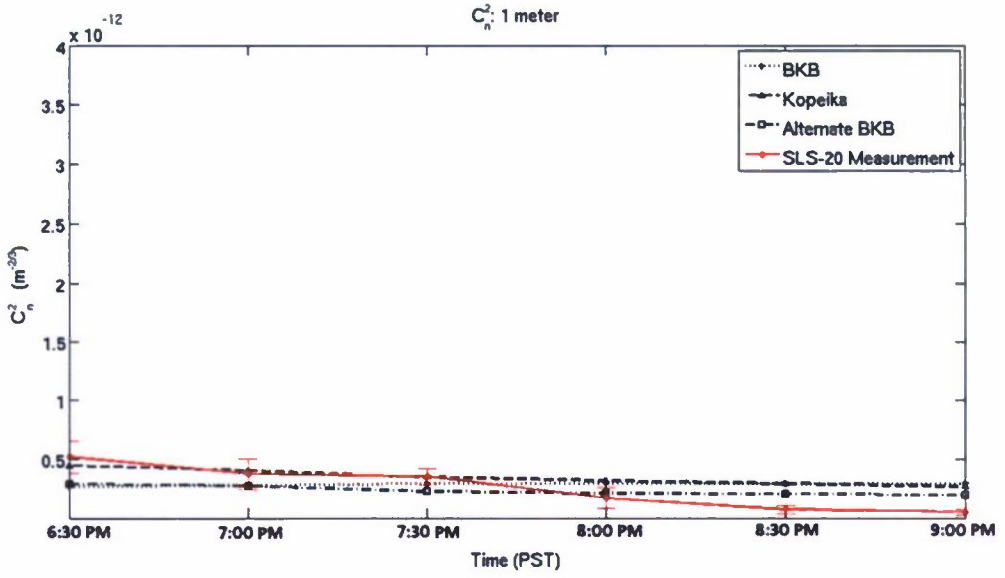

Figure 28 Comparison of C_n^2 Models 1 meter above ground (nighttime). Based on -2/3 HAP model.

As is seen in the plots above, it can be argued that the alternate BKB model fits the data more consistently than the first BKB model that was suggested. Perhaps more interestingly, the alternate BKB model demonstrates an inclination to directly follow the trend measured by the Scintec SLS-20 Scintillometers. Thus, from these results, it can be expected that direct local-measurements of macro-meteorological parameters can greatly assist in characterizing the value and trend of C_n^2 data. In particular, we have shown that the models developed by Bendersky, Kopeika, and Blaunstein [6] are applicable to a mountain environment, which can carry factors not normally observed in flat terrain. Additionally, we have also shown that the BKB models can be as accurate during evening hours as is during daytime hours. This is true provided that a -2/3 height-scaling power law is used instead of a -4/3 height-scaling power law during the evening hours. The experimental results of this proposed method demonstrate that the BKB model is an effective characterization of atmospheric turbulence, in terms of macroscopic parameters, when an alternative height-scaling method is utilized during periods of sundown.

Predictive models like those discussed here are useful for preliminary analysis of area site conditions prior to testing. Utilization of these methods allows for an accurate portrayal of atmospheric turbulence to be obtained from equipment that is relatively inexpensive, and easy to set-up and deploy. Furthermore, archived meteorological data may be utilized to reconstruct C_n^2 data in previous instances that it was not measured.

8. CONCLUDING REMARKS

In this Final Report we present results of our analysis of NGC PIF downlink data taken on Flight #1 at NTTR on May 17, 2009. We also present a similar analysis of PIF data collected in a preliminary test by NGC at PAX River on May 12, 2009. Atmospheric measurements made by UCF to characterize the atmospheric channel only took place at NTTR on May 16, 2009. Hence, all theoretical results shown for Flight #1 on May 17 are based on the assumption that conditions were similar to those on May 16. No atmospheric measurements were made at PAX River. At both testing sites, however, the Weather Research and Forecasting Model (WRF) gave estimates for Fried's parameter that permitted us to make some estimate of actual channel conditions during NGC measurements. Generally, our measurements and modeling led to slightly larger values of Fried's parameter at NTTR and at PAX River than estimated by the WRF model.

Our analysis of PIF data for Flight #1 on May 17 led to mean PIF values generally ranging from around -20 dBm at shorter ranges to -35 dBm at longer ranges (Fig. 9). By assuming moderate atmospheric conditions consistent with average conditions on May 16 characterized by the HAP model with $M = 3.3$ and $C_n^2(h_0) = 1.89 \times 10^{-13}$ m$^{-2/3}$, we produced the theoretical results shown in Fig. 9. These theoretical results were fairly consistent with much of the data. Some of the mean PIF results suggest that the AO compensation system was not always fully operational on May 17, possibly because of breakage that occurred during transport out to NTTR. The mean fade time below -41 dBm associated with Flight #1 on May 17 was often 1-2 ms or less (see Fig. 10) and we used this information to estimate packet losses for a data rate of 5 Gbps (Fig. 11).

We performed similar PIF and fade analysis on the uplink data beam from PAX River testing on May 12, 2009. In this case some of the mean PIF data for ranges less than 55 km were a few dB higher than the theoretical estimates based on transmitted power of 31.2 dBm, even after assuming that tip-tilt compensation or even full AO compensation was operational at both ends of the link (see Fig. 17). Also, the mean fade time was typically around an order of magnitude less than that at NTTR. Our conjecture for why the PAX data were better than data at NTTR is the following:

1.) Typical ranges at PAX River were shorter than those at NTTR.
2.) Background turbulence was probably much weaker at PAX River than at NTTR.
3.) Aero-optics effects were not present at PAX River because the data was taken on the uplink path.
4.) The adaptive optics compensation system appeared to be fully operational during the PAX River testing but may not have been fully operational during NTTR testing. (This conjecture is based on theoretical analysis without the benefit of actual atmospheric measurements during testing.)
5.) The propagation path at PAX River was mostly over water whereas that at NTTR was over mountains. The difference in terrains between the two sites undoubtedly led to some of the differences in the data.

We also obtained some of the IRON-T2 data taken on October 16, 2008 over a 147-km range in Hawaii. The mean PIF was typically on the order of -20 dBm and the median PIF was roughly -25 dBm.

Although not tasked to do so, we examined the theoretical mean PIF for air-to-air propagation over ranges from 10 km to 200 km to compare a full AO compensation system with no AO compensation and one that uses only tip-tilt. Our findings showed that at short ranges, the full AO system provided 1-4 dB improvement over no AO, but beyond 100 km the difference between the full AO system and no AO was 10-12 dB. At 200 km, the full AO compensation system shows improvement of roughly 3 dB over just tip-tilt at the Tx and Rx.

Our last analysis involved using macroscale measurements made at NTTR to predict C_n^2 values near the ground. The technique is based on models developed by Kopeika and colleagues [6,7] and compared against actual scintillometer measurements. We found excellent agreement between this model and our measurements at NTTR during both daytime and nighttime conditions.

9. REFERENCES

[1] L. C. Andrews, R. L. Phillips, R. Crabbs, D. Wayne, T. Leclerc, and P. Sauer, *Report: Channel Characterization for ORCA testing at NTTR*,UCF DARPA Project ID: 16296051, HR0011-08-C-0111 (September 2009).

[2] L. B. Stotts, B. Sadler, kD. Hughes, P. Kolodzy, A. Pike, D. W. Young, J. Sluz, J. Juarez, B. Graves, D. Dougherty, J. Douglass, and T. Martin, "Optical communications in atmospheric turbulence," *Proc. of SPIE* **7464**, 746403-1-17 (2009).

[3] J. M. Cicchiello, S. Harris, C. A. Pruddenc, J. Neiswenderc, D. W. Bope, C. J. Harkrider, T. G. Moore, B. Stadler , and L. Stotts "Visualizing aero-optic interactions about a nose-mounted turret," *Proc. SPIE* **7685** (2010).

[4] F. Strömqvist Vetelino, C. Y. Young, L. C. Andrews, and J. Recolons, "Aperture averaging effects on the probability density of irradiance fluctuations in moderate-to-strong turbulence," *Appl Opt.* **46** 2099-2106 (2007).

[5] D. L. Fried and H. T. Yura, "Telescope-performance reciprocity for propagation in a turbulent medium," *J. Opt. Soc. Am.* **62**, 600-602 (1972).

[6] S. Bendersky, N. S. Kopeika, and N. Blaunstein, "Atmospheric optical turbulence over land in middle east coastal environments: prediction modeling and measurements," *Appl. Opt.* **43**, 4070-4079 (2004).

[7] N. S. Kopeika, *A System Engineering Approach to Imaging,* (SPIE Press, Bellingham, 1998).

[8] D. L. Walters and K. E. Kunkel, "Atmospheric modulation transfer function for desert and mountain locations: the atmospheric effects on r_0," *J. Opt. Soc. Am.* **71**, 397-405 (1981).

[9] R. J. Noll, "Zernike polynomials and atmospheric turbulence," *J. Opt. Soc. Am.* **73**, 207-211 (1976).

APPENDIX

Additional PSD Data Sets for Flight #2 on
May 16, 2009 at NTTR

Evidence of Aero-Optic Effect on Beacon Downlink Beam: *f*×PSD